

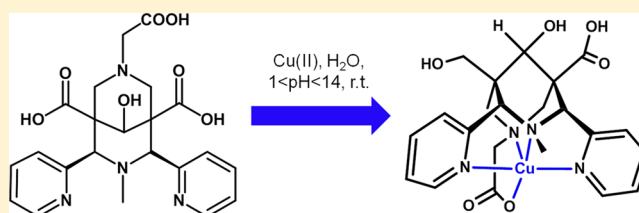
Kinetically Inert Bispidol-Based Cu(II) Chelate for Potential Application to $^{64/67}\text{Cu}$ Nuclear Medicine and Diagnosis

Amandine Roux,[†] Aline M. Nonat,^{*,†} Jérémy Brandel,[‡] Véronique Hubscher-Bruder,[‡] and Loïc J. Charbonnière^{*,†}

[†]Laboratoire d'Ingénierie Moléculaire Appliquée à l'Analyse and [‡]Laboratoire de Reconnaissance et Procédés de Séparation Moléculaire, IPHC, UMR 7178 CNRS/UdS, IPHC, UMR 7178 CNRS/UdS, ECPM, Bât R1N0, 25 rue Becquerel, 67087 Strasbourg Cedex 02, France

Supporting Information

ABSTRACT: A family of 2,4-pyridyl-disubstituted bispidol derivatives bearing methylene carboxylic acid ethyl esters (L_1 – L_3), methylene carboxylic acids (L_4 and L_5), or methylene-thiophene (L_6) groups were synthesized. In water, all ligands form rigid 1:1 complexes in the presence of Zn(II) in which the bicycle adopts a chair–chair conformation (*cis* isomer), as observed by ^1H NMR and, in the case of ligand L_1 , by an X-ray diffraction crystal structure. Interestingly, addition of Zn(II) ions on ligand L_1 induces a metal-mediated selective hydrolysis of the ethyl esters. This selective hydrolysis was not observed upon addition of other cations such as Na^+ , Mg^{2+} , and Ca^{2+} . Reduction of the central ketone was achieved to prevent ring opening via retro Diels–Alder reactions and to afford highly stable and water-soluble ligands (L_4 , L_5 , L_6). The complexation properties of L_4 and L_6 were studied in solution, with a particular interest for ligand L_4 . Fast complexation occurs in strongly acidic media (pH = 1), with a high affinity toward Cu(II) ($\log K_{\text{Cu}L_4} = 19.2(3)$, $\text{pCu} = 17.0$ at pH 7.4, $\text{pCu} = -\log[\text{Cu}_{\text{free}}]$, $[\text{Cu}] = 1 \times 10^{-6}$ M, $[\text{L}] = 1 \times 10^{-5}$ M) and high selectivity versus Co(II), Ni(II), and Zn(II), as shown by the values of the binding constants obtained from potentiometric and spectrophotometric titrations. Reversible redox potential with $E_{1/2} = -430$ mV (vs normal hydrogen electrode) was measured. The complex was found to be fairly inert from acid-assisted dissociation experiments in 5 M HClO_4 ($t_{1/2} = 110$ d at 25 °C).



INTRODUCTION

Since the PET/CT revolution in 2000 by Thomas Beyer et al.,¹ positron emission tomography (PET), combined with X-ray computed tomography (CT) scanning, currently provides some of the most accurate information on tumor distribution of many common cancers, including lymphomas and epithelial malignancies of the lung, esophagus, cervix, head, and neck. With the development of monoclonal antibodies (mAbs), engineered mAb fragments, and nontraditional antibody-like scaffolds directed against tumor targets, nuclear medical imaging is currently preparing for a new turning point in its history.² The advantages of combining antibodies and PET have previously been demonstrated: with minimal tissue attenuation and high-resolution imaging capability, immuno-PET permits improved characterization of antibody uptake in vivo and appears as a very attractive tool for the improvement and monitoring of therapy with antibody–drug conjugates.³

The major limitation that needs to be addressed comes from the fact that immuno-conjugates may display slow biodistribution kinetic, which is much longer than the radioactive half-life of commonly used positron emitters such as ^{11}C and ^{18}F ($t_{1/2} = 20$ and 110 min, respectively). Furthermore, radiochemistry with nonmetallic isotopes often necessitates demanding and complex synthesis with conditions that are not always compatible with sensitive bioconjugates. In this context,

there is an important need to develop original radioisotopes with longer half-life and simple radiochemistry.⁴

^{64}Cu ($t_{1/2} = 12.7$ h, β^+ , 17.8%, 653 keV, β^- , 38.4%, 579 keV) and ^{67}Cu ($t_{1/2} = 61.8$ h, β^- , 189 keV (20%), 154 keV (22%), 121 keV (57%)) have been identified as a promising radionuclide pair for the future of PET imaging and targeted radiotherapy for cancer.^{5,6} A large variety of ligands have been developed to satisfy the specific requirements of the radio-metals in terms of association constants, complexation kinetics, and kinetic inertness toward in vivo transmetalation and transchelation reactions.^{7–10} A majority of polyazaamacrocyclic ligands such as cyclen, cyclam, and their acetate and methylphosphonate derivatives have been used.^{11–15} DOTA and TETA display strong binding affinity for Cu; however, significant uptake was noted in the liver and kidney.^{16,17} In the case of DOTA, this has been attributed to transchelation reactions of ^{64}Cu to liver and blood proteins. However, ^{64}Cu -TETA¹⁷ and ^{64}Cu -TETA-octreotide¹⁸ showed efficient clearance through the renal system by 24 h postinjection. Significant liver retention is also observed for ^{64}Cu -NOTA.¹³

Cross-bridged DOTA and TETA demonstrate a high stability in rat serum,^{19,20} but their complexation requires

Received: January 29, 2015

Published: April 13, 2015

conditions that are often incompatible with heat-sensitive biomolecules.²¹ Other reinforced macrocyclic ligands^{22–24} as well as macrobicyclic structures such as sarcophagines^{25–27} also demonstrated very good kinetic inertness. Several other ligands based on pyridine²⁸ and picolinate units^{29–32} have been reported recently with high selectivity, fast complexation kinetics, and for a tacn-based ligand (tacn = 1,3,7-triazacyclononane),³³ a very high degree of kinetic inertness.

Previous studies on substituted bispidine (3,7-diazabicyclo[3.3.1]nonane) ligands have demonstrated that chair–chair conformers are highly preorganized and form stable complexes with transition metals^{34–37} and particularly Cu(II).^{38–40} Bispidine analogues have been shown to form stable Cu(II) complexes in water with stability constants up to $\log K_{\text{CuL}} = 18.3$ (KCl 0.1M) for ligand L_0 , as determined by 1:1:1 ligand–ligand–metal competition titrations.^{41,42} High redox potentials were measured in acetonitrile solutions, and quasi-reversible reactions were observed, pointing to a high redox stability.⁴⁰ Derivatives of L_0 with substituted pyridine groups have also been synthesized and labeled with ⁶⁴Cu. In particular, ligand L_8 was found to be particularly stable in radiolabeling challenge experiments, and biodistribution analysis in rats revealed a rapid blood and normal tissue clearance.⁴⁰ We recently reported the synthesis of three new 2,4-pyridyl-substituted bispidine derivatives substituted by methylenecarboxylic ethyl ester groups.⁴³ They feature a highly rigid bicyclic structure, either a chair–chair or a boat–chair conformation depending on the substituents in the N3 and N7 positions. In this study, methylene carboxylic acids and a methylenethiophene bispidine derivatives were synthesized, and their coordination properties with Zn(II) and Cu(II) were studied in solution and, in the case of Zn(II), in the solid state. Acid–base properties of the ligands L_4 and L_6 and the stability constants of the Co(II), Ni(II), Cu(II), and Zn(II) complexes with ligand L_4 are reported. The Cu(II) complexes with ligands L_4 and L_5 were characterized using cyclic voltammetry (CV). The kinetic stability of the Cu(II) complexes with L_4 and L_6 in acidic conditions (5 M HClO₄) was also studied.

EXPERIMENTAL SECTION

General Methods. Solvents and starting materials were purchased from Aldrich, Acros, and Alfa Aesar and used without further purification. IR spectra were recorded on a PerkinElmer Spectrum One Spectrophotometer as solid samples, and only the most significant absorption bands are given in inverse centimeters. Elemental and mass spectrometry (MS) analyses were performed by the Service Commun d'Analyses of the University of Strasbourg. ¹³C NMR spectra and two-dimensional (2D) COSY, NOESY, HSQC, and HMBC experiments were recorded on Avance 300 and Avance 400 spectrometers operating at 300 and 400 MHz, respectively. Chemical shifts are reported in ppm, with residual protonated solvent as internal reference.⁴⁴ The pH values given are corrected for the deuterium isotopic effects.⁴⁵

X-ray Crystallography. Crystals suitable for X-ray diffraction were obtained for [Zn(L₁)Cl]. The crystals were placed in oil, and a single crystal was selected, mounted on a glass fiber, and placed in a low-temperature N₂ stream. X-ray diffraction data collection was performed on a Bruker APEX II DUO Kappa-CCD diffractometer equipped with an Oxford Cryosystem liquid N₂ device, using Mo K α radiation ($\lambda = 0.71073$ Å). The crystal-detector distance was 38 mm. The cell parameters were determined (APEX2 software)⁴⁶ from reflections taken from three sets of 12 frames, each at 10 s exposure. The structure was solved by direct methods using the program SHELXS-97.⁴⁷ The refinement and all further calculations were performed using SHELXL-97.⁴⁸ The H atoms were included in

calculated positions and treated as riding atoms using SHELXL default parameters. The non-H atoms were refined anisotropically, using weighted full-matrix least-squares on F^2 . A semiempirical absorption correction was applied using SADABS in APEX2;⁴⁹ transmission factors: $T_{\text{min}}/T_{\text{max}} = 0.6981/0.7695$. The SQUEEZE instruction in PLATON was applied.⁵⁰ The residual electron density was assigned to two molecules of water solvent.

Synthesis of the Ligands. Piperidinone precursors dimethyl-1-methyl-4-oxo-2,6-di(pyridin-2-yl)piperidine-3,5-dicarboxylate (P_1)⁵¹ and dimethyl-1-carbomethoxymethyl-4-oxo-2,6-di(pyridin-2-yl)piperidine-3,5-dicarboxylate (P_2) and ligands L_1 , L_2 , and L_3 were synthesized according to previously reported procedures.⁴³

Bispidol 2₄. To a solution of L_1 (1.62 g, 3.17 mmol) in methanol (200 mL), sodium borohydride (1.20 g, 31.7 mmol) was added at 0 °C. After 30 min, the mixture was placed at room temperature for 6 d. Then, a solution of saturated NH₄Cl (10 mL) was added and, after 5 min, the solvent was removed under reduced pressure. The crude product was suspended in CH₂Cl₂ by ultrasonic treatment, and salts were eliminated by filtration. The filtrate was evaporated and solubilized in a solution of CH₃CN/0.1% trifluoroacetic acid (TFA). After evaporation, the mixture was purified by flash chromatography column on silica (dichloromethane (DCM)/MeOH, gradient 95/5 to 80/20) to obtain a pure white powder (402 mg, 23%). ¹H NMR (300 MHz, CDCl₃): δ 8.70 (multiplet, 2H, H_d+H_{d'}), 7.86 (multiplet, 2H, H_b+H_{b'}), 7.90 (d, $J = 7.8$ Hz, 1H, H_a/H_{a'}), 7.71 (d, $J = 7.8$ Hz, 1H, H_a/H_{a'}), 7.37 (multiplet, 2H, H_c+H_{c'}), 6.97 (s broad, 1H, CHOH), 5.69 (s, 1H, H₂/H₄), 5.32 (s, 1H, H₂/H₄), 4.55 (s, 1H, CHOH), 3.63 (s, 3H, OCH₃), 3.62 (s, 3H, OCH₃), 3.56 (s, 2H, CH₂CO₂Me), 3.40 (AB system, $\delta_A = 3.61$, $\delta_B = 3.18$, $J_{AB} = 11.8$ Hz, 2H, CH₂OH), 3.14 (AB system, $\delta_A = 3.37$, $\delta_B = 2.90$, $J_{AB} = 11.8$ Hz, 2H, H₆/H₈), 2.78 (AB system, $\delta_A = 2.94$, $\delta_B = 2.61$, $J_{AB} = 11.8$ Hz, 2H, H₆/H₈), 2.36 (s, 3H, CH₃). ¹³C NMR (75 MHz, CDCl₃): δ 168.0 (CO₂Me), 167.4 (CO₂Me), 149.6 (C_{py}), 148.8 (C_{py}), 147.4 (C_d/C_{d'}), 146.9 (C_d/C_{d'}), 135.4 (C_b/C_{b'}), 135.3 (C_b/C_{b'}), 125.5 (C_a/C_{a'}), 123.6 (C_a/C_{a'}), 122.0 (C_c+C_{c'}), 69.1 (C₉), 64.8 (C₂/C₄), 63.9 (C₂/C₄), 60.9 (CH₂OH), 53.8 (CH₂CO₂Me), 50.8 (C₆/C₈), 50.2 (OCH₃), 50.1 (C₁), 50.0 (C₆/C₈), 49.9 (OCH₃), 41.0 (CH₃), 40.7 (C₅). Electrospray ionization (ESI)/MS⁺ (CH₂Cl₂): $m/z = 471.22$ ([M + H]⁺, 100%). Anal. Calcd for C₂₄H₃₀O₆N₄NaCl·CH₃OH: C, 53.52, H, 6.11, N, 9.99. Found: C, 53.88, H, 5.88, N, 10.05%.

Ligand L₄. Bispidine 2₄ (40.0 mg, 0.09 mmol) was solubilized in H₂O (3 mL), and NaOH (10.8 mg, 0.27 mmol) was added. The mixture was stirred at room temperature during 5 d, and the solvent was evaporated to dryness under vacuum. The solid was dissolved in a minimum of H₂O and precipitated by addition of tetrahydrofuran (THF, 4 mL). The resulting precipitate was collected by centrifugation and dried under vacuum. 1 M HCl was added, and the mixture was purified by filtration on a C18 reverse-phase column with methanol to obtain L₄·2HCl·4NaCl·4H₂O (168 mg, 24%). ¹H NMR (300 MHz, D₂O): δ 8.69 (multiplet, 2H, H_d+H_{d'}), 7.81 (m, 1H, H_b/H_{b'}), 7.78 (m, 1H, H_b/H_{b'}), 7.34 (multiplet, 4H, H_c+H_{c'}+H_a+H_{a'}), 4.35 (s, 1H, H₂), 4.03 (s broad, 2H, H₄+H₆), 3.22 (AB system, $\delta_A = 3.57$, $\delta_B = 2.87$, $J_{AB} = 10.9$ Hz, 2H, CH₂CO₂H), 2.76 (AB system, $\delta_A = 2.84$, $\delta_B = 2.68$, $J_{AB} = 7.9$ Hz, 2H, CH₂OH), 2.23 (AB system, $\delta_A = 2.65$, $\delta_B = 1.80$, $J_{AB} = 11.2$ Hz, 2H, H₈/H₆), 2.36 (AB system, $\delta_A \approx 2.84$, $\delta_B = 1.88$, $J_{AB} = 12.3$ Hz, 2H, H₈/H₆), 1.76 (s, 3H, CH₃). ¹³C NMR (75 MHz, D₂O): δ 180.0 (CH₂CO₂H), 178.9 (CO₂H), 159.0 (C_{py}), 158.5 (C_{py}), 150.0 (C_d/C_{d'}), 149.6 (C_d/C_{d'}), 137.2 (C_b/C_{b'}), 137.0 (C_b/C_{b'}), 125.7 (C_c/C_{c'}), 124.9 (C_c/C_{c'}), 123.1 (C_a/C_{a'}), 123.0 (C_a/C_{a'}), 72.3 (C₉), 68.2 (C₂+C₄), 64.7 (CH₂OH), 64.2 (CH₂CO₂H), 56.4 (C₈/C₆), 55.5 (C₆/C₈), 51.3 (C₁), 42.8 (CH₃), 42.1 (C₅). IR (cm⁻¹, ATR) ν 3257 (broad, $\nu_{\text{O-H}}$ alcohol), 3037, 2699 (broad, $\nu_{\text{O-H}}$ carboxylic acid), 1723 (s, $\nu_{\text{C=O}}$ acid), 1536, 1464 (m, $\nu_{\text{C=C}}$ aromatic). ESI/MS⁺ (H₂O): $m/z = 443.20$ ([M + H]⁺, 100%). Anal. Calcd for C₂₂H₂₆O₆N₄·2HCl·4NaCl·4H₂O: C, 32.17, H, 4.42, N, 6.82. Found: C, 32.18, H, 4.07, N, 6.81%. The purity was confirmed by potentiometry and ¹H NMR titration with a reference of known concentration;⁵² in that case *p*-dimethylaminopyridine was used.

Bispidine 1₅. In a solution of methanol (14 mL), glycine (538.0 mg, 7.17 mmol) and NaHCO₃ (604.0 mg, 7.17 mmol) were mixed

under magnetic stirring during 2 h at 45 °C. Formaldehyde (1.46 mL, 19.6 mmol) and piperidinone P₁ (2.5 g, 6.52 mmol) in methanol (20 mL) were added at room temperature, and the mixture was stirred under reflux during 5 h. Solvents were removed under reduced pressure, and the obtained solid was crystallized in ethanol (26 mL). A precipitate was obtained upon slow evaporation at room temperature. Pure compound **1₅** was obtained as a white powder after filtration (1.63 g, 52%). ¹H NMR (300 MHz, CDCl₃): δ 8.91 (multiplet, 2H, H_d), 7.65 (dd, J₁ = 7.8 Hz, J₂ = 7.4 Hz, 2H, H_b), 7.22 (d, J = 7.4 Hz, 2H, H_a), 7.20 (dd, J₁ = 8.2 Hz, J₂ = 7.8 Hz, 2H, H_c), 4.66 (s, 2H, H₂), 3.72 (s, 6H, OCH₃), 3.02 (s, 2H, CH₂CO₂H), 3.13 (AB system, δ_A = 3.53, δ_B = 2.73, J_{AB} = 12.3 Hz, 4H, H₈), 2.14 (br s, 1H, CO₂H), 1.97 (s, 3H, CH₃). ¹³C NMR (100 MHz, CDCl₃): δ 203.1 (C=O), 174.5 (CO₂H), 168.1 (CO₂Me), 156.4 (C_{py}), 151.4 (C_d), 137.4 (C_a), 124.5 (C_b/C_c), 124.1 (C_b/C_c), 73.0 (C₂), 63.5 (CH₂CO₂H), 59.2 (C₈), 52.9 (OCH₃), 43.5 (CH₃), 36.9 (C₁). IR (cm⁻¹, ATR) ν 3369 (broad, ν_{O-H} acid), 1752 (m, ν_{C=O} ester), 1732 (s, ν_{C=O} acid), 1591 (s, ν_{C=C} aromatic). ESI/MS⁺ (CH₂Cl₂): m/z = 483.19 ([M + H]⁺, 100%). Anal. Calcd for C₂₄H₂₅O₇N₄Na₂·2.5H₂O: C, 52.46, H, 5.50, N, 10.20. Found: C, 52.38, H, 5.58, N, 10.37%.

Bispidol 2₅. Bispidone **1₅** (2.50 g, 5.20 mmol) was dissolved in anhydrous methanol (100 mL) and was cooled at -77 °C in an acetone/dry ice bath. Sodium borohydride (0.30 g, 7.80 mmol) was slowly added. After 6 h at -77 °C, a solution of saturated NH₄Cl (20 mL) was added, and the mixture was stirred during 10 min. After evaporation of the solvent, the mixture was suspended in dichloromethane and filtered, and TFA (150 μL) was added to the filtrate. Solvents were removed under reduced pressure affording **2₅** (2.50 g, 94%). ¹H NMR (400 MHz, CD₃OD): δ 8.80 (d, J = 1.8 Hz, 2H, H_d), 7.94 (dd, J₁ = 7.8 Hz, J₂ = 1.9 Hz, 2H, H_c), 7.77 (d, J = 7.8 Hz, 2H, H_a), 7.51 (dd, J = 7.6 Hz, 2H, H_b), 5.57 (s, 2H, H₂), 4.43 (s, 1H, H₉), 3.72 (s, 6H, OCH₃), 3.67 (s, 2H, CH₂CO₂H), 3.29 (AB system, δ_A = 3.51, δ_B = 3.06, J_{AB} = 12.3 Hz, 4H, H₈), 2.32 (s, 3H, CH₃). ¹³C NMR (100 MHz, CD₃OD): δ 173.5 (CH₂CO₂H), 170.6 (CO₂Me), 153.0 (C_{py}), 151.0 (C_d), 139.0 (C_a), 128.6 (C_b/C_c), 126.1 (C_b/C_c), 73.5 (C₉), 67.1 (C₂), 56.9 (C₈), 54.1 (CH₂CO₂H), 53.7 (C₅), 53.3 (OCH₃), 43.8 (CH₃). ESI/MS⁺ (MeOH): m/z = 485.20 ([M + H]⁺, 100%).

Ligand L₅. Bispidine **2₅** (86 mg, 0.18 mmol) was dissolved in H₂O/THF (4 mL/4 mL), and sodium hydroxide (43 mg, 1.07 mmol) was added. The mixture was stirred during 4 d. The solvent was removed under reduced pressure. Ligand L₅ was obtained after purification on column chromatography (reverse phase, H₂O/CH₃CN 100% to 80/20) as a sodium salt (50 mg, 40%). ¹H NMR (400 MHz, D₂O): δ 8.61 (dd, J₁ = 5.0 Hz, J₂ = 1.78 Hz, 2H, H_d), 7.72 (dd, J₁ = 7.7 Hz, J₂ = 1.9 Hz, 2H, H_b), 7.39 (d, J = 7.7 Hz, 2H, H_a), 7.31 (dd, J₁ = 7.4 Hz, J₂ = 5.1 Hz, 2H, H_c), 4.52 (s, 2H, H₂), 3.96 (s, 1H, H₉), 2.88 (s, 2H, CH₂CO₂H), 2.57 (AB system, δ_A = 2.94, δ_B = 2.11, J_{AB} = 12.2 Hz, 4H, H₈), 1.77 (s, 3H, CH₃). ¹³C NMR (100 MHz, D₂O): δ 179.0 (CO₂H), 178.8 (CO₂H), 159.6 (C_{py}), 149.3 (C_{py}), 136.9 (C_{py}), 125.9 (C_{py}), 122.7 (C_{py}), 74.2 (C₉), 67.5 (C₂), 65.0 (CH₂CO₂H), 56.9 (C₈), 51.8 (C₁), 42.8 (CH₃). ESI/MS (positive mode): m/z = 479.15 ([M + Na]⁺, 100%), 480.16 ([M + Na]⁺, 23.8%). Anal. Calcd for C₂₂H₂₁O₇N₄Na₃·2NaCl·4H₂O: C, 37.14, H, 4.11, N, 7.88. Found: C, 37.61, H, 4.38, N, 7.52%.

Bispidone 1₆. Piperidinone P₁ (497.0 mg, 1.3 mmol) was dissolved in warm methanol (6 mL), and formaldehyde (290 μL, 3.9 mmol) was added after the solution cooled at room temperature. After 10 min, 2-aminomethylthiophene (147 μL, 1.43 mmol) was added to the mixture, and the reaction was warmed at 55 °C during 2 h 30 min under stirring. Slow evaporation gave a precipitate that was filtered and washed with cold methanol affording **1₆** (290.0 mg, 43%). ¹H NMR (300 MHz, CD₃OD): δ 8.45 (d, J = 4.9 Hz, 2H, H_d), 7.98 (d, J = 7.9 Hz, 2H, H_a), 7.59 (t, J = 7.7 Hz, 2H, H_b), 7.38 (d, J = 5.3 Hz, 1H, H₉), 7.16 (dd, J₁ = 7.5 Hz, J₂ = 4.7 Hz, 2H, H_c), 6.97 (dd, J₁ = 5.1 Hz, J₂ = 3.2 Hz, 1H, H₁), 6.88 (d, J = 3.2 Hz, 1H, H_e), 4.72 (s, 2H, H₂), 3.83 (s, 6H, OCH₃), 3.57 (s, 2H, CH₂thiophen), 2.82 (AB system, δ_A = 3.06, δ_B = 2.57, J_{AB} = 12.7 Hz, 4H, H₈), 2.01 (s, 3H, CH₃). ¹³C NMR (75 MHz, CD₃OD): δ 203.7 (C=O), 168.7 (CO₂Me), 158.7 (C_{py}), 149.1 (C_d), 139.5 (C_{thiophen}), 136.5 (C_b), 128.4, (C_e), 127.1 (C_f), 125.7 (C_g),

123.7 (1_d), 123.0 (C_c), 73.8 (C₂), 62.2 (C₁), 58.8 (C₈), 55.6 (CH₂thiophen), 52.7 (OCH₃), 43.4 (CH₃). IR (cm⁻¹, ATR) ν 1734 (s, ν_{C=O} ester), 1716 (m, ν_{C=O} ketone), 1589, 1571 (w, ν_{C=C} aromatic), 1280 (s, ν_{C=O}). ESI/MS⁺ (MeOH): m/z = 521.18 ([M + H]⁺, 100%). Anal. Calcd for C₂₇H₂₈O₅N₄S: C, 62.29, H, 5.42, N, 10.76. Found: C, 62.14, H, 5.53, N, 10.98%.

Bispidol 2₆. Bispidone **1₆** (960 mg, 1.84 mmol) was dissolved in anhydrous methanol (80 mL) and was cooled to -77 °C in an acetone/dry ice bath. Sodium borohydride (106 mg, 2.77 mmol) was slowly added. After 3 h 30 min at -77 °C, a solution of saturated NH₄Cl (20 mL) was added in the flask, and the mixture was stirred during 30 min. After evaporation of the solvent, the mixture was suspended in DCM and filtered, and TFA (150 μL) was added in the filtrate. Solvents were removed under reduced pressure, and the obtained solid was purified by column chromatography (SiO₂; DCM/MeOH 95/5–75/25). Slow evaporation at room temperature gave the pure product as white crystals (410 mg, 43%). ¹H NMR (400 MHz, CD₃OD): δ = 8.50 (d, J = 4.8 Hz, 2H, H_d), 7.88 (d, J = 7.8 Hz, 2H, H_a), 7.77 (t, J = 7.8 Hz, 2H, H_b), 7.39 (d, J = 5.2 Hz, 1H, H₉), 7.30 (dd, J₁ = 7.5 Hz, J₂ = 4.8 Hz, 2H, H_c), 7.04 (dd, J₁ = 5.3 Hz, J₂ = 3.6 Hz, 1H, H₁), 6.99 (d, J = 3.3 Hz, 1H, H_e), 5.90 (s, 2H, H₂), 4.61 (s, 1H, H₉), 3.96 (s, 2H, CH₂thiophen), 3.68 (s, 6H, OCH₃), 3.15 (AB system, δ_A = 3.37, δ_B = 2.93, J_{AB} = 12.3 Hz, 4H, H₈), 2.26 (s, 3H, CH₃). ¹³C NMR (100 MHz, CD₃OD): δ = 169.4 (CO₂Me), 152.5 (C_{py}), 149.4 (C_d), 137.5 (C_b+C_{thiophen}), 128.6 (C_e), 128.2 (C_a), 127.0 (C_f), 126.5 (C_g), 124.3 (C_c), 73.0 (C₉), 65.9 (C₂), 55.0 (CH₂thiophen), 54.4 (C₈), 53.1 (C₁), 52.4 (OCH₃), 42.7 (CH₃). ESI/MS⁺ (MeOH): m/z = 523.2029 ([M + H]⁺, 100%).

Ligand L₆. Compound **2₆** (309 mg, 0.59 mmol) was dissolved in THF (32 mL), and sodium hydroxide (71 mg, 1.78 mmol) in H₂O (12 mL) was added. The solution was stirred at room temperature during 6 d. After evaporation, hydrochloric acid (5 mL) was added, and after 1 h, solvent was removed under reduced pressure. Product was purified by filtration on a reverse-phase column (100% H₂O then 80:20 H₂O/MeOH) to yield L₆·0.3HCl as a white powder (210 mg, 74%). ¹H NMR (400 MHz, CD₃OD): δ 8.62 (d, J = 3.8 Hz, 2H, H_d), 7.92 (t, J = 7.6 Hz, 2H, H_b), 7.72 (d, J = 5.2 Hz, 1H, H₉), 7.52–7.40 (multiplet, 5H, H_c+H_a+H_e), 7.25 (multiplet, 1H, H₁), 4.94 (s, 2H, H₂), 4.50 (s, 2H, CH₂thiophen), 4.37 (s, 1H, H₉), 3.41 (AB system, δ_A = 3.65, δ_B = 3.16, J_{AB} = 12.6 Hz, 4H, H₈), 1.91 (s, 3H, CH₃). ¹³C NMR (100 MHz, D₂O, 50 °C): δ 179.1 (CO₂H), 161.7 (C_{py}), 148.3 (C_d), 137.3 (C_b/C_{thiophen}), 137.3 (C_b+C_{thiophen}), 128.8 (C_e), 127.7 (C_a), 126.3 (C_f), 125.7 (C_g), 123.0 (C_c), 75.0 (C₉), 68.7 (C₂), 56.8 (CH₂thiophen), 56.5 (C₈), 51.7 (C₁), 43.4 (CH₃). IR (cm⁻¹, ATR) ν 3240 (broad, ν_{O-H} alcohol), 3056 (broad, ν_{O-H} acid), 1710 (m, ν_{C=O} acid), 1590 (s, ν_{C=C} aromatic). ESI/MS⁻ (H₂O): m/z = 493.16 ([M - H]⁻, 100%). Anal. Calcd for C₂₅H₂₆O₅N₄S·0.3HCl: C, 59.40, H, 5.24, N, 11.08. Found: C, 59.14, H, 5.44, N, 10.81%.

Synthesis and Characterization of the Complexes. [ZnL_n*Cl]

To a solution of ligand L₁ (306.0 mg, 0.60 mmol) in THF (20 mL) was added ZnCl₂ (109 mg, 0.78 mmol) dissolved in H₂O (3 mL). The mixture was stirred for 24 h at room temperature and evaporated under reduced pressure. The solid was dissolved in a minimum of H₂O (6 mL), and addition of a large volume of THF (75 mL) resulted in the formation of a precipitate, which was collected by centrifugation and dried under vacuum to give the complex [ZnL₁*Cl]·2H₂O (300 mg, 82%). ¹H NMR (300 MHz, D₂O): δ 8.67 (d, J = 5.0 Hz, 2H, H_d), 8.10 (t, J = 7.9 Hz, 2H, H_b), 7.70 (t, J = 6.5 Hz, 2H, H_c), 7.50 (d, J = 7.9 Hz, 2H, H_a), 5.18 (s, 2H, H₂), 3.75 (s, 6H, OCH₃), 3.12 (s, 2H, CH₂COO⁻), 2.84 (AB system, δ_A = 3.07, δ_B = 2.60, J_{AB} = 13.1 Hz, 4H, H₈), 2.16 (s, 3H, CH₃). ¹³C NMR (75 MHz, D₂O): δ 177.4 (COO⁻), 169.8 (COOMe), 152.9 (C_{py}), 149.1 (CH_{py}), 142.7 (CH_{py}), 126.3 (CH_{py}), 125.4 (CH_{py}), 92.7 (C₉), 68.1 (C₂), 61.2 (CH₂COO⁻), 55.9 (C₁), 54.1 (C₈), 53.6 (OCH₃), 44.0 (CH₃). ESI/MS⁺(H₂O): m/z = 563.11 ([M]⁺, 100%), 545.10 ([M-H₂O]⁺, 100%), 547.10 ([M-H₂O]⁺, 58%), 549.10 ([M-H₂O]⁺, 42%). Anal. Calcd for ZnC₂₄H₂₇O₈N₄Cl₂H₂O: C, 45.37, H, 4.76, N, 8.82. Found: C, 45.36, H, 4.77, N, 8.81%.

All of the following zinc complexes were prepared in situ in D₂O by mixing appropriate amounts of ligand and metal as the zinc chloride salt.

[ZnL₄]. Ligand L₄ (10.4 mg, 0.024 mmol) and ZnCl₂ (4.8 mg, 0.028 mmol) were dissolved in D₂O (0.7 mL). ¹H NMR (300 MHz, D₂O): δ 8.65 (m, 2H, H_d+H_{d'}), 8.10 (m, 2H, H_b+H_{b'}), 7.74 (d, J = 7.9 Hz, 1H, H_a/H_{a'}), 7.67 (m, 2H, H_c+H_{c'}), 7.60 (d, J = 7.9 Hz, 1H, H_a/H_{a'}), 5.04 (s, 1H, H₂/H₄), 4.45 (s, 1H, H₂/H₄), 4.36 (s, 1H, H₆), 3.45 (AB system, δ_A = 3.72, δ_B 3.17, J_{AB} = 11.4 Hz, 2H, CH₂CO₂H/H₈/H₆), 3.08 (AB system, δ_A = 3.13, δ_B = 3.03, J_{AB} = 17.5 Hz, 2H, CH₂CO₂H/H₈/H₆), 2.77 (AB system, δ_A = 2.88, δ_B = 2.66, J_{AB} = 13 Hz, 2H, CH₂CO₂H/H₈/H₆), 2.48 (s, 2H, CH₂OH), 2.10 (s, 3H, CH₃). ¹³C NMR (75 MHz, D₂O): δ 177.9 (CH₂CO₂⁻), 173.0 (CO₂⁻), 154.3 (C_{py}), 154.0 (C_{py}), 148.9 (C_d/C_{d'}), 148.6 (C_d/C_{d'}), 141.0 (C_b/C_{b'}), 140.7 (C_b/C_{b'}), 126.8 (C_a/C_{a'}), 126.4 (C_a/C_{a'}), 125.9 (C_c+C_{c'}), 69.8 (C₉), 65.0 (C₂/C₄), 64.0 (C₂/C₄), 62.7 (CH₂CO₂⁻), 61.1 (CH₂OH), 57.3 (C₈/C₆), 57.1 (C₈/C₆), 51.9 (C₁/C₅), 43.9 (C₁/C₅), 42.9 (CH₃). High-resolution ESI/MS⁺ (H₂O) calcd for C₂₂H₂₅O₆N₄Zn: m/z = 505.1060 [M]⁺, 100%. Found: 505.1050.

[Zn1₆Cl₂]. ZnCl₂ (3.8 mg, 0.028 mmol) was added to a solution of bispidone I₆ (11.1 mg, 0.021 mmol) in THF (2.0 mL) and stirred overnight at room temperature. The mixture is evaporated to dryness and dissolved in D₂O (0.7 mL). ¹H NMR (300 MHz, D₂O): δ 8.84 (d, J = 5.2 Hz, 2H, H_d), 8.18 (t, J = 7.8 Hz, 2H, H_b), 7.80 (dd, J₁ = 7.7 Hz, J₂ = 5.3 Hz, 2H, H_c), 7.57 (d, J = 7.8 Hz, 2H, H_a), 7.45 (d, J = 5.1 Hz, 1H, H_g), 7.06 (dd, J₁ = 5.1 Hz, J₂ = 3.3 Hz, 1H, H_f), 6.98 (d, J = 3.3 Hz, 1H, H_b), 5.20 (s, 2H, H₂), 4.23 (s, 2H, CH₂thiophen), 3.75 (s, 6H, OCH₃), 2.76 (AB system, δ_A = 3.03, δ_B = 2.49, J_{AB} = 13.4 Hz, 4H, H₈), 2.19 (s, 3H, CH₃). ¹³C NMR (75 MHz, D₂O): δ = 169.9 (CO₂CH₃), 153.4 (C_{py}), 148.9 (C_d), 142.1 (C_b), 132.0 (C_e), 130.6 (C_{thiophen}), 128.1 (C_g), 127.5 (C_f), 126.6 (C_c), 126.0 (C_a), 92.6 (C₉), 68.3 (C₂), 55.5 (CH₂thiophen), 55.2 (C₁), 53.7 (OCH₃), 50.0 (C₈), 45.6 (CH₃). ESI/MS⁺ (H₂O): m/z = 637.09 [M+Cl]⁺.

[ZnL₆]. Ligand L₆ (15.0 mg, 0.03 mmol) and ZnCl₂ (7.0 mg, 0.04 mmol) were dissolved in D₂O (0.7 mL). ¹H NMR (300 MHz, D₂O): δ 8.62 (d, J = 5.2 Hz, 2H, H_d), 7.92 (t, J = 7.8 Hz, 2H, H_b), 7.72 (d, J = 7.9 Hz, 2H, H_c), 7.52 (t, J₁ = 7.4 Hz, J₂ = 5.1 Hz, 2H, H₂), 7.45 (d, J = 5.2 Hz, 1H, H_g), 7.06 (t, J₁ = 5.2 Hz, J₂ = 3.4 Hz, 1H, H_f), 7.02 (d, J = 3.3 Hz, 1H, H_e), 5.06 (s, 2H, H₂), 4.25 (s, 2H, CH₂thiophen), 4.22 (s, 1H, H₆), 2.79 (AB system, δ_A = 2.89, δ_B = 2.69, J_{AB} = 13.2 Hz, 4H, H₈), 2.15 (s, 3H, CH₃). ¹³C NMR (75 MHz, D₂O): δ 172.8 (CO₂H), 154.4 (C_{py}), 148.5 (C_d), 141.4 (C_b), 132.1 (C_e), 130.8 (C_{thiophen}), 128.1 (C_g), 127.5 (C_f), 127.5 (C_a), 126.1 (C_c), 71.2 (C₉), 63.7 (C₂), 55.7 (CH₂thiophen), 53.1 (C₈), 50.9 (C₁), 45.1 (CH₃). ESI/MS⁺: m/z = 593.05 [M+Cl]⁺.

Physicochemical Studies. Materials. Distilled water was purified by passing through a mixed bed of ion-exchanger (Bioblock Scientific R3–83002, M3–83006) and activated carbon (Bioblock Scientific ORC-83005). All the stock solutions were prepared by weighing solid products using an AG 245 Mettler Toledo analytical balance (precision 0.01 mg). Metal cation solutions were prepared from their perchlorate salts (Cu(ClO₄)₂·6H₂O, 98%, Fluka; Zn(ClO₄)₂·6H₂O, 98.9%, Alfa Aesar; Co(ClO₄)₂ 98%, Fluka; and Ni(ClO₄)₂·6H₂O, 98%, Aldrich), and their concentrations were determined by colorimetric titrations with ethylenediaminetetraacetic acid (1 × 10⁻² M, Merck, Titriplex III) according to standard procedures.⁵³ Sodium hydroxide (NaOH) and perchloric acid (HClO₄) were used to adjust pH during titrations. The ionic strength of all the solutions was fixed to 0.1 M with potassium chloride (KCl, Fluka, 99.0%). All the experiments described were repeated at least three times.

Caution! Perchlorate salts combined with organic ligands are potentially explosive and should be handled in small quantities and with the adequate precautions.⁵⁴

Potentiometry. The protonated species of L₄ and L₆ and the stability constants of L₄ complexes with Cu(II), Zn(II), Co(II), and Ni(II) complexes were characterized and quantified by potentiometric titrations in water. All the solutions used in the potentiometric experiments were prepared from boiled and degassed water. Titrations were performed using an automatic titrator system (DMS 716 Titrino, Metrohm) with a combined glass electrode (Metrohm, 6.0234.100,

Long Life) filled with NaCl 0.1 M. The electrode was calibrated as a hydrogen concentration probe by titrating known amounts of perchloric acid with CO₃²⁻ free sodium hydroxide solutions. The GLEE program^{55,56} was used for the glass electrode calibration.

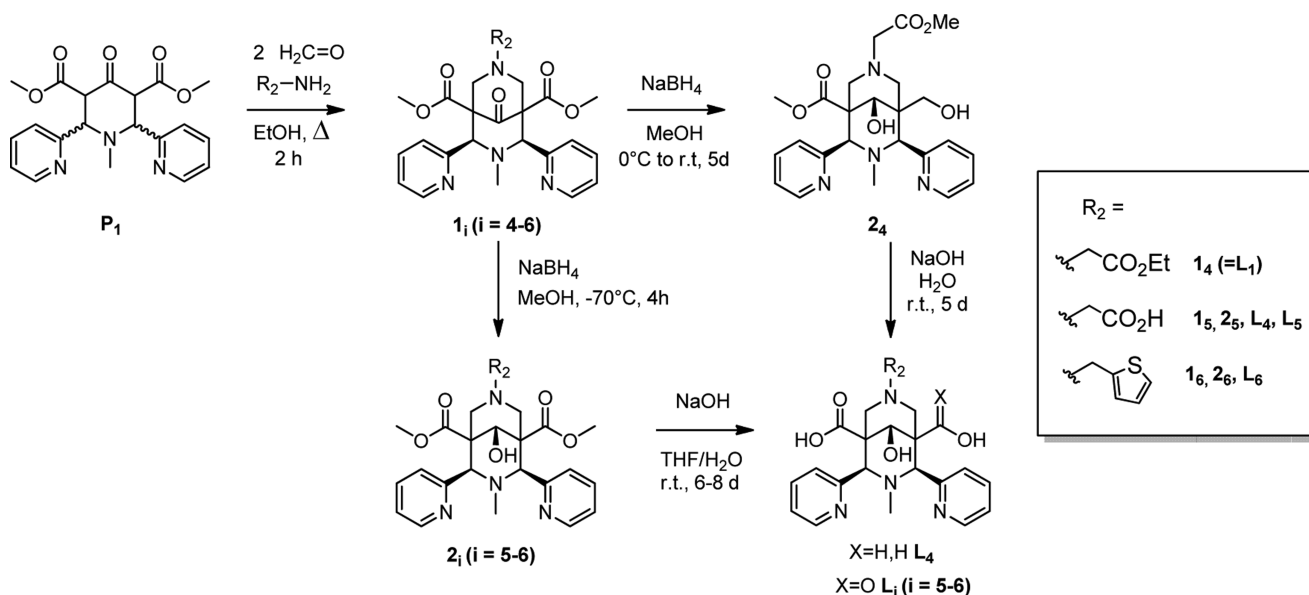
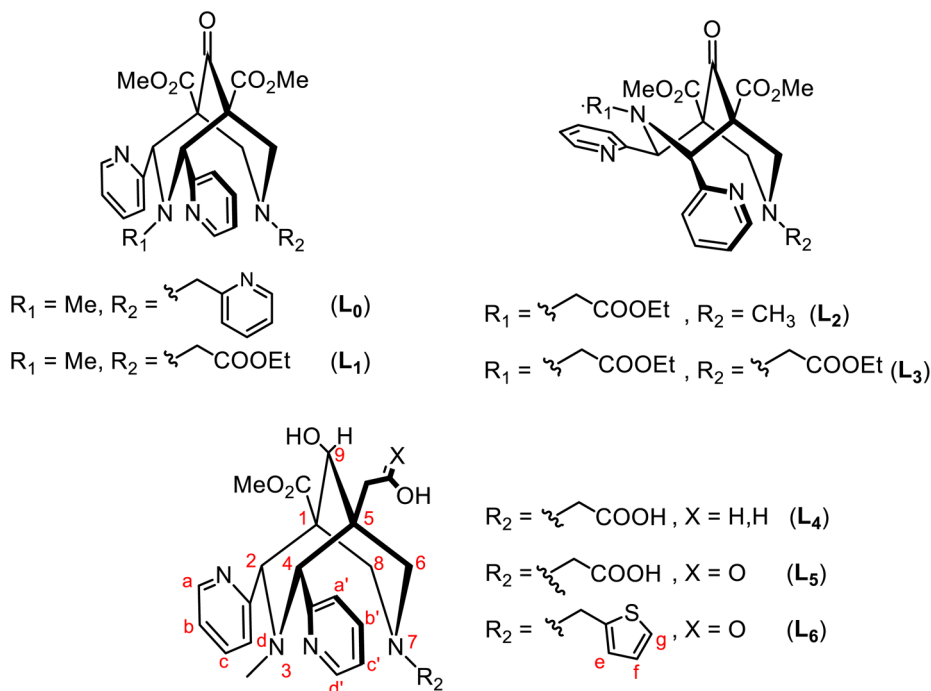
In a typical experiment, an aliquot of 10 mL of L (1 × 10⁻³ M) or M/L (M = Zn(II), Co(II), or Ni(II), [M]/[L] ≈ 1) was introduced into a thermostated jacketed cell (25.0(2) °C, Metrohm) and kept under argon during the titrations. The solutions were acidified with a known volume of HClO₄, and the titrations were then performed by addition of known volumes of sodium hydroxide solution over the pH range of 2–12. The potentiometric data of L and its metal complexes were refined with the Hyperquad 2008 program,⁵⁷ which uses nonlinear least-squares methods, taking into account the formation of metal hydroxide species. The titration of each system was repeated at least in triplicate, and the sets of data for each system were treated independently, then merged together and treated simultaneously to give the final stability constants. The distribution curves as a function of pH of the protonated species of L₄ and L₆ and of L₄ and L₆ metal complexes were calculated using the Hyss2009 program.⁵⁸

Spectrophotometry. The protonation constants of L₄ and L₆ and the stability constants of M/L (M = Cu(II), Zn(II), Co(II), and Ni(II) for L₄ and M = Cu(II) for L₆, [M]/[L] = 1, [L] ≈ 1 × 10⁻⁴ M) were also determined by UV–visible spectrophotometric titration versus pH by recording simultaneously pH and UV–visible spectra. Since complexation started in very acidic medium, the titrations were performed in two different ways. Between pH = 0 and pH = 2, batch solutions were prepared. Each sample was prepared separately by mixing a known amount of L stock solution, a known amount of standardized HClO₄ to adjust the pH (pH = -log[H⁺]), and a known amount of Cu(II) stock solution in the case of the study of the complexes ([Cu(II)]/[L] = 1). Between pH 2 and 12.5, direct titrations were performed. Typically, an aliquot of 10 mL of L solution was introduced into a thermostated jacketed cell (25.0(2) °C) with 1 equiv of metal (M) in the case of M/L titrations. A known volume of perchloric acid solution was added to adjust the pH to 2, and the titrations were performed by addition of known volumes of potassium hydroxide solution. The free hydrogen ion concentrations were measured with a Mettler Toledo U402–S7/120 (pH 0–14) combined glass electrode. Potential differences were given by a Tacussel LPH430T millivoltmeter. Standardization of the millivoltmeter and verification of the linearity of the electrode were performed with three commercial buffer solutions (pH 4.01, 7.01, and 10.01; 25 °C).

For all the spectrophotometric titrations, UV–visible absorption spectra versus pH were recorded in 1 cm quartz Suprasil cells using a Varian (Cary 3) spectrophotometer equipped with a thermoregulated cell compartment (25.0(2) °C). The software SPECFIT Global Analysis System V3.0 32 bit for Windows was used to determine the coordination model and calculate the stability constants (log β) of the formed species.⁵⁹

Acid Decomplexation Studies. Acid-decomplexation studies were performed under pseudo-first-order conditions on a 5.48 × 10⁻⁵ mM solution of Cu(II)L₄ complex and on a 4.97 × 10⁻⁵ mM solution of Cu(II)L₆ complex in 5 M HClO₄ at 25 °C. Changes in the absorption spectra with time were monitored using a PerkinElmer Lambda 950 spectrophotometer. The decomplexation reaction was monitored by following the ratio A_{263 nm}/A_{273 nm} over time during four months.

Cyclic Voltammetry. CV was performed on the CuL₄ and CuL₅ complexes at room temperature with a Radiometer Analytical MDE150/PST50 interfaced to a personal computer. The CV experiments were performed using a glassy carbon working electrode (0.071 cm², BASi). The electrode surface was polished routinely before use. The counter electrode was a Pt coil, and the reference electrode was a Ag/AgCl electrode. The CuL complex was measured in Ar-degassed water with ionic strength fixed at 0.1 M with KCl, at five different values of pH (pH = 2.38, 4.30, 7.34, 9.36, 11.49) and different scan rates (50–300 mV/s).

Scheme 1. Synthesis of Bispidine Ligands L_4 , L_5 , and L_6 .Chart 1. Structure of Bispidone (L_1 – L_3) and Bispidol (L_4 – L_6) Ligands Discussed in This Work

RESULTS AND DISCUSSION

Synthesis and Structural Characterization of the Ligands. Two-step synthesis of bispidones L_1 – L_3 (bispidone = 9-oxo-3,7-diazabicyclo[3.3.1]nonane) was achieved according to the procedures we previously reported.⁴³ Bispidones 1_5 and 1_6 (Scheme 1) were obtained via double Mannich reactions from the piperidinone P_1 , formaldehyde, and the corresponding amine, that is, glycine (1_4 and 1_5) and 2-(aminomethyl)-thiophen (1_6) (see Supporting Information, Figures S1–S2 for the ^1H NMR spectra of 1_5 and 1_6). Reduction of the as-obtained bispidone into the corresponding bispidol (2_4 , 2_5 , and 2_6) was achieved with NaBH_4 . Reduction of the ketone was necessary to stabilize the bispidine skeleton and prevent ring opening via retro-Mannich mechanism in acidic condition, as

well as decarboxylation of the β -keto acid. Selective reduction of the central ketone of bispidones 1_5 and 1_6 was achieved upon addition of 1.5 equiv of NaBH_4 in cold methanol (-70°C). As a comparison, the reduction reaction was performed in the presence of an excess of NaBH_4 (10 equiv) and at higher temperature (0°C to room temperature) with ligand L_1 , and in that case, partial reduction of the methyl ester substituent was also observed. Bispidine 2_4 was isolated, in which one methyl ester group was reduced with a concomitant trans-esterification of the ethyl acetate substituent into a methyl ester. Finally, saponification of the methyl ester groups was performed to obtain water-soluble ligands (L_4 , L_5 , and L_6 , Scheme 1).

The conformation of the bicyclic ring, as well as the configuration of the pyridyl substituents of the final ligands and

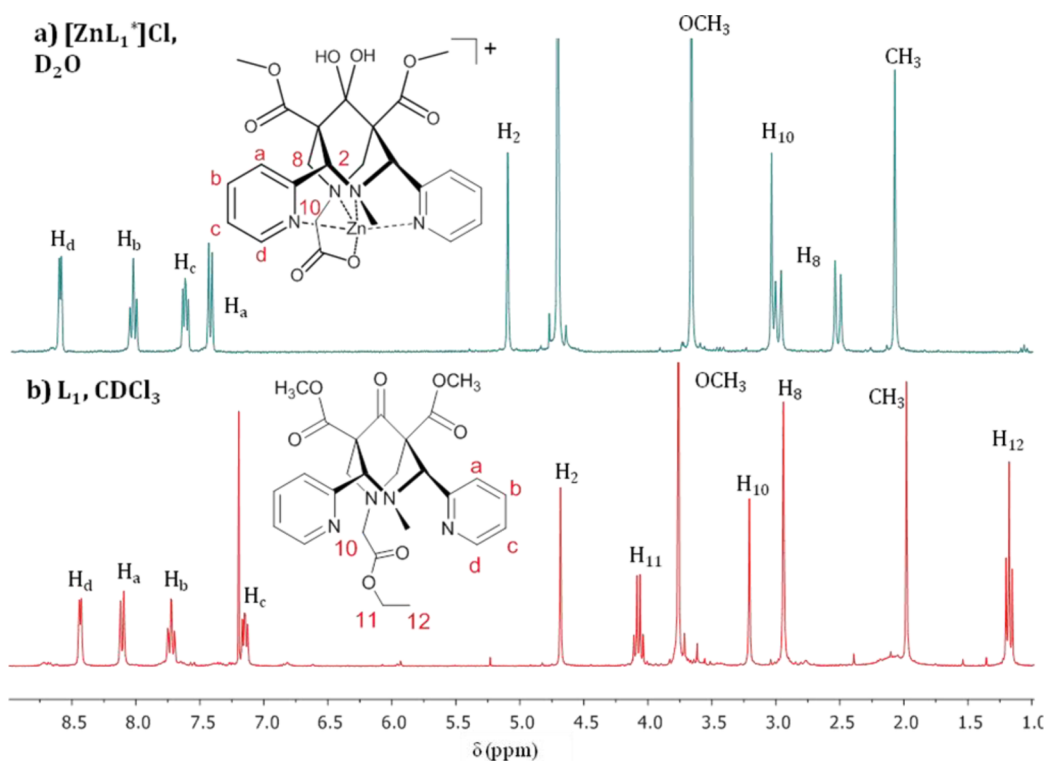
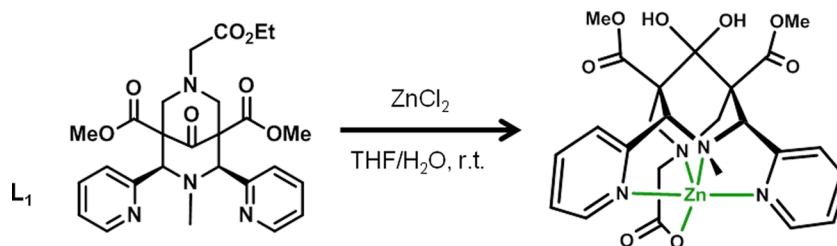


Figure 1. (a) ^1H NMR spectrum of the isolated complex $[\text{ZnL}_1^*]\text{Cl}$ (300 MHz, D_2O , 25 °C). (b) ^1H NMR spectrum of L_1 (300 MHz, CDCl_3 , 25 °C).

Scheme 2. Synthesis of $[\text{ZnL}_1^*]\text{Cl}$ ^a



^aWhere L_1^* is the gem-diol form of the ketone L_5 .

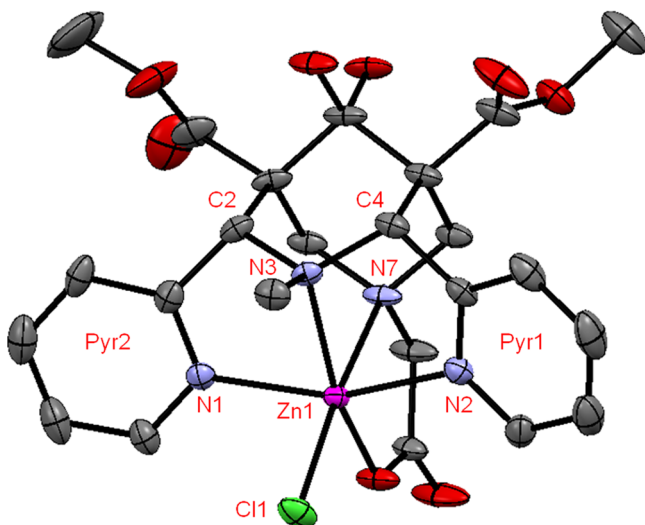


Figure 2. ORTEP diagram of the complex $[\text{ZnL}_1^*]\text{Cl}$ with thermal ellipsoids at 30% probability.

the intermediates was determined by NMR studies. 2D-COSY (^1H – ^1H and ^1H – ^{13}C) experiments combined with ^1H – ^1H NOESY experiment allowed the accurate assignment of all signals (see Supporting Information, Figures S3–S5 for the ^1H NMR spectra of L_4 , L_5 , and L_6). Bispidine L_1 , L_4 , L_5 , and L_6 , and the corresponding intermediates, were isolated in a chair–chair conformation, with the pyridyl substituents in the equatorial position, leading to highly preorganized compounds with cis-symmetrical configuration, well-adapted for the coordination of metal ions. After reduction, the hydroxyl group is pointing toward N_3 , as confirmed by the presence of nuclear Overhauser effects between the proton atom in position 9 (see Chart 1 for atom numbering) and the proton atoms of the second cycle (H_8/H_6) in ^1H – ^1H NOESY experiments (Supporting Information, Figure S6). In conclusion, this method allows achieving selective reduction with controlled stereochemistry in a reproducible manner. As a comparison, previous reports describe the selective reduction of the central ketone in the presence of a large excess of NaBH_4 (7 equiv) in a mixture of dioxane and water, but depending on the substituent in R_2 , either the same epimer was isolated ($\text{R}_2 =$

Table 1. Crystallographic Data for the Structures of L_1 and $[ZnL_1^*]Cl$

formula	L_1^a	$[ZnL_1^*]Cl$
	$C_{26}H_{30}N_4O_7$	$C_{24}H_{27}ClN_4O_8Zn$
molecular weight ($g\ mol^{-1}$)	510.54	600.32
temperature (K)	173(2)	173(2)
crystal size (mm)	0.30 × 0.25 × 0.20	0.35 × 0.30 × 0.25
crystal system	monoclinic	monoclinic
space group	$P2_1/c$	$P2_1/c$
unit-cell dim (\AA , deg)	$a = 14.8091(4)$ $b = 11.8613(4)$ $c = 14.8551(4)$ $\beta = 100.775(2)$	$a = 9.0749(2)$ $b = 16.9463(4)$ $c = 17.5698(4)$ $\beta = 106.3810$
volume (\AA^3); Z	2563.37(13); 4	2592.31(10); 4
density (calcd, $g\ cm^{-3}$)	1.323	1.538
abs. coeff (mm^{-1})	0.097	1.106
$F(000)$	1080	1240
θ_{max}	27.46	31.98
reflections collected	25 582	35 134
independent reflections	5860	9008
$I > 2\sigma(I)$ reflections	4496	7992
parameters	338	348
R1, wR2 ($I > 2\sigma(I)$)	0.0566, 0.1418	0.0631, 0.1443
R1, wR2 (all data)	0.0832, 0.1555	0.0693, 0.1462

^aFrom ref 43.**Table 2.** Selected Bond Lengths and Angles in L_1 , $[ZnL_1^*]Cl$, and $[ZnL_0(H_2O)](BF_4)_2$

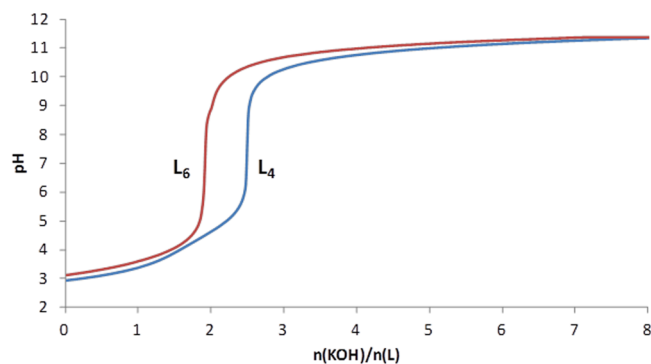
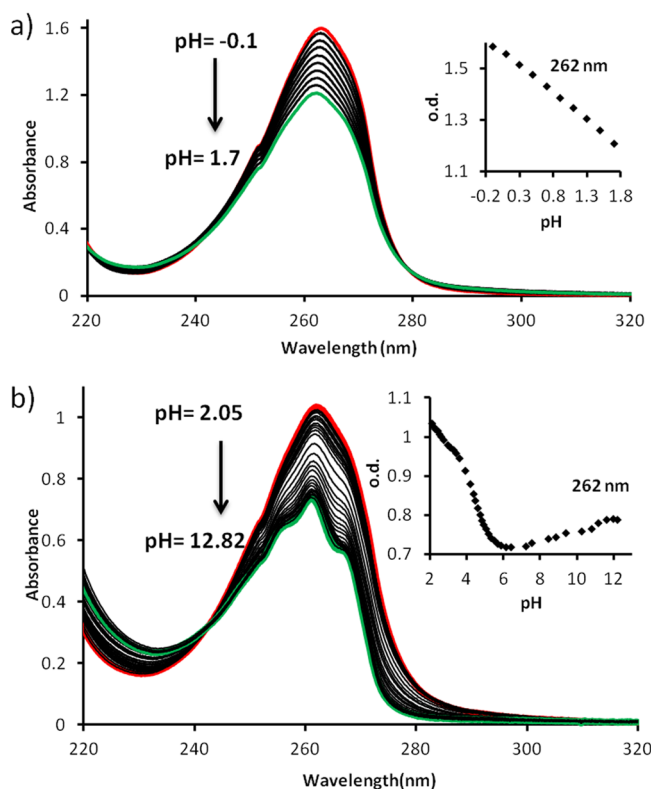
	L_1^a	$[ZnL_1^*]Cl$	$[ZnL_0(H_2O)](BF_4)_2^b$
bond lengths and distances (\AA)			
Zn–N7	2.349(3)		2.248(6)
Zn–N3	2.181(3)		2.220(6)
Zn–N1	2.135(3)		2.124(6)
Zn–N2	2.159(3)		2.140(6)
Zn–Y	2.026(2) (Y = O)		2.089(6) (Y = N)
Zn–X	2.373(1) (X = Cl) Cl		2.200(5) (X = O)
$\sum_i (Zn-N_i, Y)$	10.82		10.85
N3...N7	2.89	2.92	2.94
Pyr1...Pyr2	7.19	6.75	4.14
angles (deg)			
N3–Zn–N7	91.7		82.1
N7–Zn–Y	78.8 (Y = O)		95.7 (Y = N)
Y–Zn–N1	102.9		152.4
Pyr1...Pyr2	159.8	153.19	152.4

^aFrom ref 43. ^bFrom ref 63.

methyl,⁶⁰ benzyl⁶¹) or the other epimer with H_9 pointing toward N_3 (R_2 = methyl(pyridine),³⁸ ethyne, ethanethiol⁴⁰).

As stated in our previous report,⁴³ a boat–chair conformation was observed in methanol for the bispidine L_2 and L_3 , associated with trans configuration of the pyridine rings. The important stabilization of the trans isomer in these systems was explained by the presence of different weak hydrogen-bonding interactions between the ethyl acetate substituent on N_3 and the pyridyl rings at C_2 and C_4 or $C(sp^3)$ –H groups.

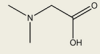
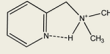
Coordination Properties of the Zn(II) Complexes. *Structural Characterization by 1H NMR.* The coordination properties of ligands L_1 – L_6 were studied by 1H NMR, using Zn(II) as a diamagnetic metal ion. In all cases, addition of 1.1

**Figure 3.** Potentiometric titration of L_4 and L_6 . $[L_4]_{tot} = 1.00 \times 10^{-3}$ M ($2.12 \leq pH \leq 11.49$) and $[L_6]_{tot} = 9.64 \times 10^{-4}$ M ($2.38 < pH < 11.69$); solvent: H_2O ; $I = 0.1$ M (KCl); $T = 25.0(2)$ °C.**Figure 4.** Spectrophotometric titration of L_4 vs pH. (a) Batch titration, $[L_4]_{tot} = 9.81 \times 10^{-4}$ M, $-0.1 < p[H] < 1.7$. (b) Direct titration, $[L_4]_{tot} = 1.01 \times 10^{-4}$ M, $2.05 \leq p[H] \leq 12.82$ (H_2O ; $I = 0.1$ M (KCl); $T = 25.0(2)$ °C).

equiv of zinc chloride in a solution of ligand in CD_3OD is associated with marked changes associated with coordination.

As expected from the boat–chair conformation of ligands L_2 and L_3 , which is unadapted to metal complexation, a complex mixture of species was observed by 1H NMR. However, the 1H NMR spectra of L_1 , L_4 , L_5 , and L_6 in the presence of stoichiometric amount of Zn(II) show only one set of signals, associated with significant changes in the protons chemical shifts, pointing to the formation of a rigid 1:1 complex in solution (Figure 1 and Supporting Information, Figures S3–S5). In all cases, the coordination of the nitrogen atoms of the pyridine substituents induces a significant shielding of the protons H_a , being displaced into the magnetic anisotropy cone of the O atoms of the methyl esters. Moreover the coordination

Table 3. Successive Protonation Constants of L₄ and Relevant Selected Ligands^a

log K _n ^H		L ₄	L ₆		
log K ₁ ^H	N _{tert}	> 12	> 12	/	/
log K ₂ ^H		10.6(6)	11.8(2)	10.54 ⁷⁷	/
log K ₃ ^H	COOH	4.5(1)	3.6(1)	/	/
log K ₄ ^H		2.0(2)	2.3(3)	1.93 ⁷⁷	/
log K ₅ ^H	Pyridines	0.82(1)	0.62(7)	/	0.9
log K ₆ ^H		< 0.82	< 0.62	/	/

^aH₂O, I = 0.1 M (KCl), T = 25.0 °C. The numbers in parentheses correspond to the standard deviations expressed as the last significant digit.

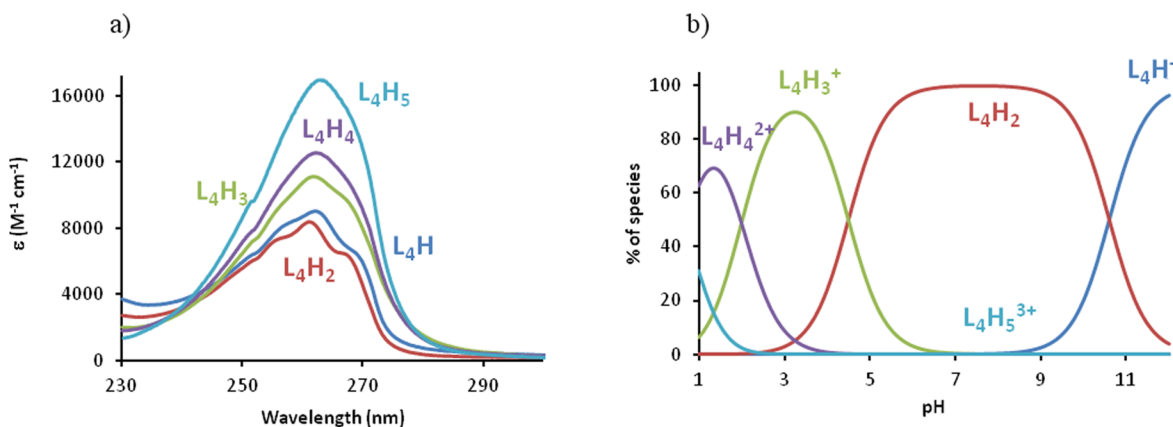


Figure 5. (a) Electronic spectra and (b) distribution diagram of the protonated species of L₄ ([L₄]_{tot} = 1.0 × 10⁻⁴ M, H₂O, I = 0.1 M KCl, T = 25.0(2) °C).

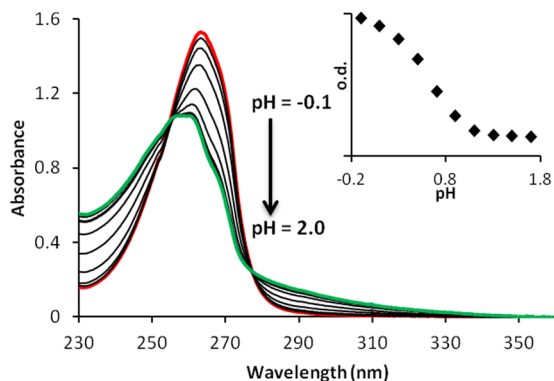


Figure 6. Spectrophotometric titration of CuL₄ vs pH. [L₄]_{tot} = 9.81 × 10⁻⁵ M, [Cu(II)]_{tot}/[L₄]_{tot} = 1, -0.1 < pH < 2.0, H₂O, I = 0.1 M (NaClO₄), T = 25.0(2) °C). (inset) Spectral variations at 261 nm as a function of calculated pH.

of the nitrogen atom N₃ induces a strong deshielding of the protons H₂ and H₄. Finally, a significant increase of the coupling constant (1 Hz) of the AB spin system of protons H₆/H₈ is observed and accounts for the stiffening of the skeleton in the Zn(II) complexes.

In the case of L₁, selective hydrolysis of the ethyl ester function was clearly observed upon addition of Zn(II) in CD₃OD, which was accompanied by the disappearance of the ethyl ester quadruplet at δ = 4.16 ppm and the appearance of a new signal at δ = 3.72 ppm, accounting for the CH₂ protons of ethanol (Supporting Information, Figure S7). Monitoring this reaction with time allowed us to identify a mechanism in three steps: (i) first, coordination with Zn(II), (ii) trans-esterification

Table 4. Overall Stability Constants (log β) of the ML₄ Complexes

stability constant ^a	Cu	Zn	Ni	Co
log β _{ML₄}	19.2(3) ^b	14.45(2) ^c	12.2(3) ^{b,c}	11.1(2) ^{b,c}
log β _{ML₄H}			16.7(2) ^{b,c}	15.02(3) ^c
log β _{ML₄OH}			3.4(4) ^{b,c}	

^aM = Cu(II), Zn(II), Co(II), Ni(II), H₂O; I = 0.1M; T = 25.0 °C, β_{MLH} = [MLH]/([M][L][H]); charges were omitted for clarity; log K_{Cu(OH)} = -6.29; log K_{Cu(OH)₂} = -13.1; log K_{Zn(OH)} = -7.89; log K_{Zn(OH)₂} = -14.92; log K_{Ni(OH)} = -8.1; log K_{Ni(OH)₂} = -16.87 (from ref 83); log K_{Co(OH)} = -6.35 (from ref 84). ^bSpectrophotometry. ^cPotentiometry. Stability constants of hydroxo species were considered.

of the ethyl ester with CD₃OD, and (iii) hydrolysis of the obtained methyl ester. This selective hydrolysis was not observed upon addition of other cations such as Na⁺, Mg²⁺, and Ca²⁺. Such catalytic effect of the zinc ion is not surprising since most zinc enzymes act as hydrolases and often catalyze the hydrolysis of ester bonds.⁶² To avoid any secondary species due to incomplete trans-esterification or hydrolysis, the synthesis of the Zn(II) complex was performed in a mixture of THF and H₂O (Scheme 2). The corresponding ¹H NMR spectrum is presented in Figure 1. Full assignment of the signals was achieved by ¹H-¹H COSY and NOESY experiments (Supporting Information, Figure S8). Overhauser effects were observed between the CH₃ protons and the protons H₂/H₄, confirming their axial position. Through-space dipolar coupling was also observed between the pyridyl protons H₃ and the axial proton H₂/H₄ as well as the OCH₃ protons,

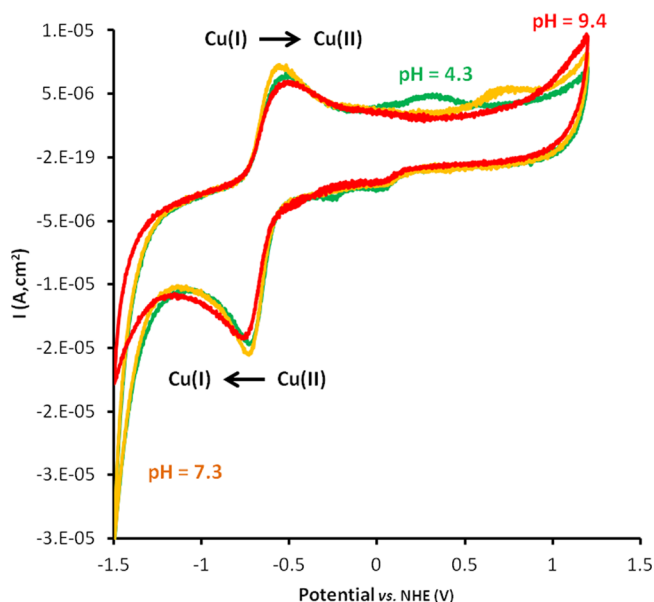


Figure 7. Cyclic voltammograms of CuL_4 at different pH ($V = 200$ mV/s). $[\text{CuL}_4] = 9.07 \times 10^{-4}$ M, H_2O , $I = 0.1$ M (NaClO_4), $T = 25.0(2)^\circ\text{C}$.

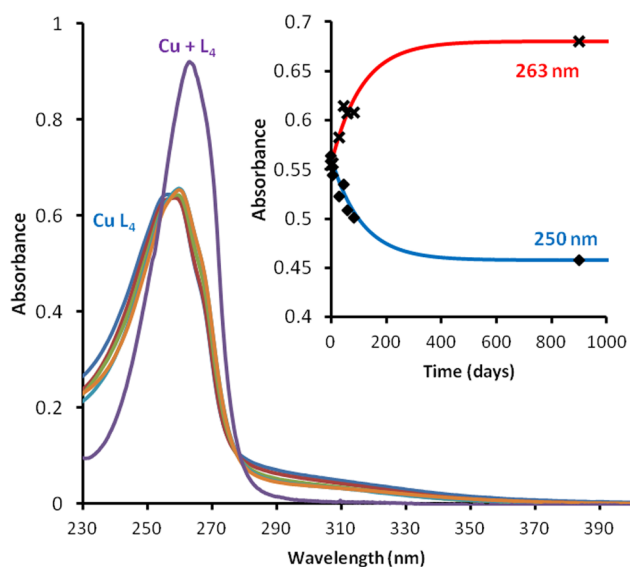


Figure 8. Evolution of the absorption spectra of CuL_4 in 5 M HClO_4 over four months at 25°C at 0 (blue), 6 (red), 31 (green), 59 (turquoise), and 84 days (orange) and of a solution of free Cu(II) and L_4 in the same conditions (purple) ($[\text{CuL}_4] = 5.48 \times 10^{-5}$ M). (inset) Evolution of the absorbance upon time (experimental data point and fit).

confirming the reorientation of the pyridyl substituents in the syn conformation upon complexation. Interestingly, hydration of the central ketone is favored upon complexation, as observed by ^{13}C NMR with a chemical shift at 93 ppm corresponding to a gem-diol (L_1^*) instead of 203 ppm for the ketone in the spectrum of the ligand. This was further confirmed by the crystal structure of the complex in the solid state (Figure 2).

Solid-State Structure of the Complex $[\text{ZnL}_1^*]\text{Cl}$. X-ray quality crystals of the Zn(II) complex formed with ligand L_1 were obtained by slow evaporation of a solution of isolated $[\text{ZnL}_1^*]\text{Cl}\cdot 2\text{H}_2\text{O}$ complex in methanol at room temperature. The ORTEP diagram of $[\text{ZnL}_1^*]\text{Cl}$ is shown in Figure 2, and

the corresponding crystallographic data are presented in Tables 1 and 2.

The Zn(II) ion is hexacoordinated by ligand L_5 and one chloride counterion (Figure 2). As for other transition-metal complexes with pentadentate bispidone ligands^{63–65} the coordination sphere can be described as an octahedral geometry with tetragonal distortion. As expected, the geometry of the rigid diazabicyclononane skeleton is only faintly modified upon coordination of Zn(II) , and in particular the N1–N2 distance remains almost unchanged (Table 2). The major structural changes upon coordination arise from the rotation of the pyridine substituents at C2 and C4 and the hydrolysis of the ethyl ester, providing a strongly coordinating carboxylate donor. Moreover, hydration of the central ketone is observed, confirming previous NMR data. The values of Zn–N3 and Zn–N7 are very similar to the values found for complex $[\text{ZnL}_0](\text{BF}_4)_2$ where the acetate substituent is replaced by a methylpyridyl substituent.⁶³ However, little changes are observed in the Zn–N1 and Zn–N2 distances, with the Zn(II) center slightly shifted toward N7, probably due to a stronger coordination of the carboxylate donor in comparison to the pyridyl moiety.

Physicochemical Studies. Protonation Constants of the Ligands L_4 and L_6 . Ligands L_4 and L_6 (Chart 1) possess six protonation sites: two tertiary amines, two pyridine nitrogen atoms, and two carboxylic acid functions. Protonation constants, as defined by eqs 1 and 2, were determined by a combination of potentiometric (Figure 3) and UV–vis absorption spectrophotometric titrations versus pH (Figure 4 and Supporting Information, Figure S9).



$$K_n^{\text{H}} = \frac{[\text{LH}_n]}{[\text{LH}_{n-1}][\text{H}]} \quad n = 1 - 6 \quad (2)$$

Because of the known strong stability of the metal complexes of bispidine derivatives,^{42,39} ligands L_4 , L_6 , and their Cu(II) complexes were studied in strongly acidic conditions. Between $\text{pH} = 0$ and $\text{pH} = 2$, the batch titration technique was used (Figure 4a), and the pH of the solutions was fixed by adding known volumes of standardized HClO_4 (see Experimental Section for details). Note that the ionic strength was not fixed in the batch titrations and that no decomposition of the ligands was observed, even in strongly acidic conditions. Direct titrations on L_4 and L_6 were also performed in the pH range of 2–12 (Figure 4b). The spectrophotometric titrations versus pH of L_4 showed one band, centered at 260 nm, attributed to the $\pi\text{--}\pi^*$ transition of the pyridine rings, which underwent hypochromic variation and showed shoulders appear upon increase of the pH.⁶⁶ The hypochromic variation in very acidic conditions is typical of the deprotonation of pyridinium nitrogens.^{67,68} The shoulders appearing in basic conditions suggest the existence of hydrogen bonding with at least one pyridine nitrogen lone pair.⁶⁹ Ligand L_6 shows the same band plus an additional large band centered around 240 nm due to the presence of the thiophene moiety (Figure S9).⁷⁰

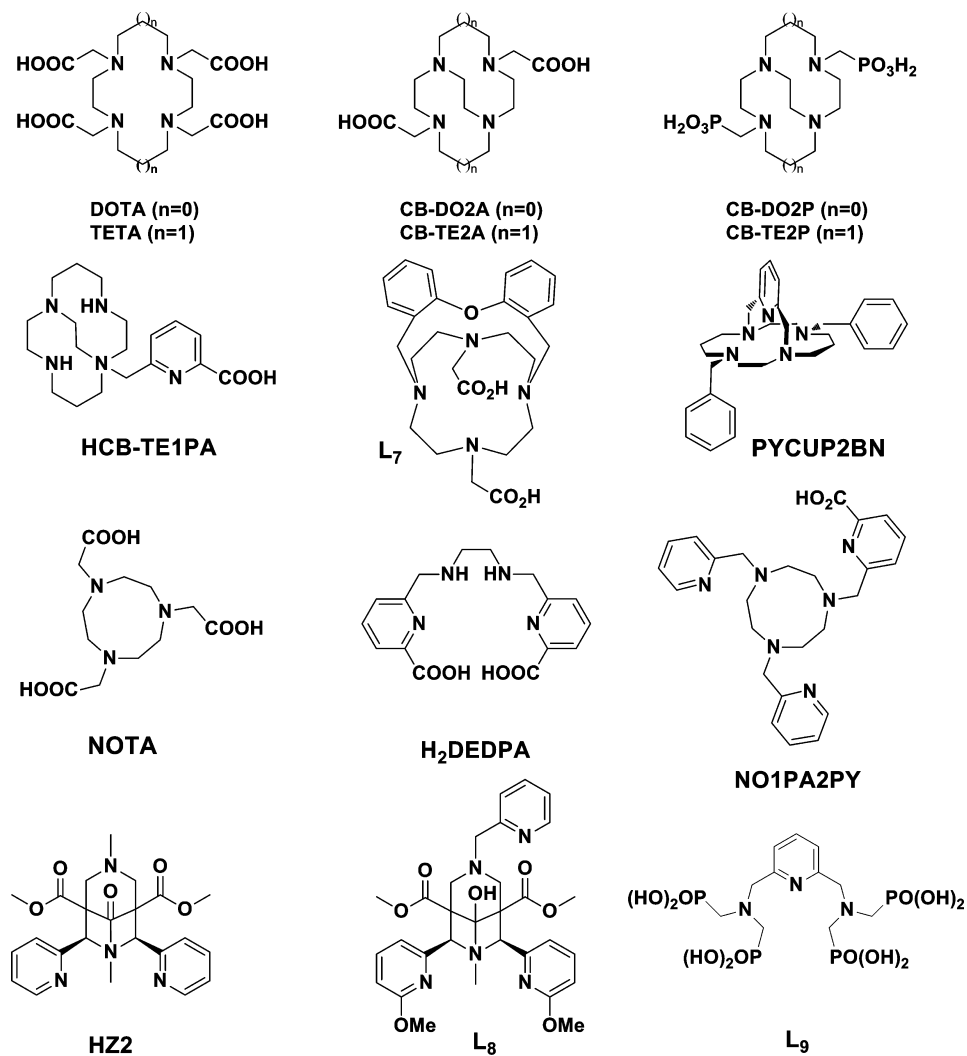
The statistical analysis of the potentiometric and spectrophotometric data versus pH was achieved with Hyperquad2008^{71,57} and Specfit32,^{72,59} respectively, and led to the determination of four protonation constants of ligand L_4 and L_6 in the pH range from 0 to 12 (Table 3). The first two protonation constants (K_1^{H} and K_2^{H}), with $\log K$ higher than 10, were assigned to the tertiary amines of the bispidine

Table 5. Calculated pM^a ($M = \text{Cu(II)}, \text{Zn(II)}, \text{Ni(II)}$) Values, Half Life ($t_{1/2}$), and Reduction Potential (E_{red}) for L_4 and Other Relevant Ligands from Literature

	pCu	pZn	pCo	pNi	$t_{1/2}$	E_{red} (mV)/NHE	radiolabeling conditions
L_4	17.0	12.2	10.6	10.0	71 d (5 M HClO_4 , 25 °C)	-560	
L_6	15.9				46 d (5 M HClO_4 , 25 °C)		
HZ2 ⁴²	15.8	10.6	6.0			-225	
L_0 ⁴²	18.9	8.9	6.9	6.9		-323 (E^0)	
cyclam ²¹	20.8				3.8 min (5 M HCl, 90 °C)	-480 (irr)	
NOTA9	18.4				<3 min (5 M HCl, 30 °C)		25 °C, 30–60 min, pH 5.5–6.5
TETA5	15.1				3.5 d (5 M HCl, 30 °C)		25 °C, 60 min, pH 5–7
NO1PA2PY ³³	17.75	13.28			204 min (3 M HCl, 90 °C)	-518	r.t., 30 min, pH 6–7
L_7 ²³	12.11	5.06			30.8 d (12 M HCl, 90 °C)	-447, -591 (irr)	
L_8 ⁴⁰							r.t., 1 min, pH 5.5
L_9 ^{79,80}	15.5	11.1	9.2	10.1			
CB-TE2A ^{9,20}					154 h (5 M HCl, 90 °C)	-880 ($E_{1/2}$)	95 °C, 60 min, pH 6–7
CB-TE2P ^{13,88}					3.8 h (5 M HCl, 90 °C)	-760	r.t., 30 min, pH 8.1
HCB-TE1PA ³⁰	16.6				96 d (5M, HClO_4 , 25 °C)	-620	
H_2DEDPA ²⁹	18.5				<5 min (6 M HCl, 90 °C)	-920 (irr)	25 °C, 5–10 min, pH 5.5
PYCUP2BN ²²					20.3 h (5 M HCl, 90 °C)		70 °C, 15 min, pH 7.4

^a $pM = -\log[M(\text{II})_{\text{free}}]$, $[M] = 1 \times 10^{-6}$ M, $[L] = 1 \times 10^{-5}$ M.

Chart 2. Structure of Other Ligands Discussed in This Work



skeleton.^{41,73–75} K_2^{H} was attributed to the N_7 nitrogen of the bispidine backbone by comparison with dimethylglycine (Table 3), while the other tertiary amine (N_3) was too basic to be

deprotonated in our pH range. The third and fourth protonation constants ($K_3^{\text{H}}, K_4^{\text{H}}$) were attributed to the two carboxylic acid oxygens. In the case of L_4 , by comparison with

dimethylglycine, we suggest that K_4^H is attributed to the methylcarboxylic acid on N7, and thus K_3^H is attributed to the carboxylic acid on C1. The two most acidic protonation constants belong to the pyridine nitrogens. Only one could be determined from our spectrophotometric batch titrations, and its value ($\log K_5^H$) is in agreement with the protonation of the pyridine group of *N,N'*-dimethyl(pyridine-2-yl)methylamine (Table 3).⁷⁶

From these values, the electronic spectra of the protonated species of L_4 (Figure 5) and L_6 (Supporting Information, Figure S10) and their distribution diagram were calculated.⁷⁷ The distribution curves showed that only the neutral zwitterionic diprotonated species L_4H_2 and L_6H_2 are present under physiological conditions (pH 7.4). These data also confirm the attribution of the first two protonations to the tertiary amines. Indeed, the shape and absorption coefficient of the calculated UV-absorption spectra of L_4H^- and L_4H_2 (L_4H^- , $\epsilon_{260} = 8730 \text{ M}^{-1}\cdot\text{cm}^{-1}$ and L_4H_2 , $\epsilon_{260} = 8210 \text{ M}^{-1}\cdot\text{cm}^{-1}$) is very similar to the protonated form of *N,N'*-dimethyl(pyridine-2-yl)methylamine ($\epsilon_{260} \approx 3700 \text{ M}^{-1}\cdot\text{cm}^{-1}$) taking into account the presence of two pyridines in L_2 .

Determination of the Stability Constants of the Cu(II) Complexes. Upon spectrophotometric titration of a solution of L_4 and Cu(II) ($[\text{Cu(II)}]/[L_4] = 0.92$) between pH = 2 and 12, both the ligand bands (Supporting Information, Figure S11) and the Cu(II) d–d bands (Supporting Information, Figure S13) showed no spectral variations. Both the shape of the ligand bands (significantly different from the free ligand spectra) and the position of the d–d band (660 nm) suggest that the Cu(II) complex is already formed at pH = 2 and exhibits a square pyramidal geometry.⁷⁸ This was also confirmed by the titration of ligand L_4 upon addition of a Cu(II) solution at pH = 2 (Supporting Information, Figure S12). The thermodynamic stability constant ($\log \beta_{\text{Cu}L_4} = 19.2(3)$) was determined from the variations of the UV–visible absorption spectra of a Cu(II)/ L_4 1:1 solution between pH ($-\log[\text{H}^+]$) -0.1 and 1.7 , using batch technique (Figure 6). Significant changes were seen in the absorption spectrum of L_4 as a function of pH, where the hypo- and hypsochromic shift of the main band at 260 nm together with the appearance of a small charge transfer band^{66,79,80} indicated the complete formation of the complex at pH = 1.3.

Unlike L_4 , the complexation of Cu(II) by ligand L_6 is characterized by a slow complexation kinetic at room temperature, and marked changes in the UV–visible absorption spectra can be observed over a period from 1 to 2 h. Complexation was monitored by UV–visible spectrophotometry using the batch technique in the pH range from -0.3 to 1.9 (Supporting Information, Figure S14). These titrations also showed that a unique Cu(II) complex is formed from very low pH (pH > 0.8), in agreement with a strong binding constant ($\log \beta_{\text{Cu}L_6} = 19.4(1)$). The maximum absorption of the d–d transitions was centered at 630 nm in that case, suggesting similar square pyramidal coordination geometry to $\text{Cu}L_4$ (Supporting Information, Figure S15). Moreover, significant variations at 240 nm, corresponding to the $\pi-\pi^*$ transition of the thiophene, suggested its implication in the Cu(II) coordination sphere (Figure S14).

Selectivity of L_4 for Cu(II) Versus Co(II), Ni(II), and Zn(II). To avoid the release of the radioisotope in vivo due to transmetalation, ^{64}Cu chelates should present an important selectivity for Cu(II) over other metals. We focused our attention on the study of the complexation of Zn(II) since it is

the most abundant bioavailable cation, and solid states and ^1H NMR studies pointed to a good affinity of our ligands for Zn(II). Ni(II) was also studied since it is the main species obtained during the production of ^{64}Cu from enriched ^{64}Ni targets by cyclotron, the ratio of metal Ni to ^{64}Cu being in the order of millions.^{81,9} Co(II) is also observed, coming either from a side nuclear reaction (^{61}Co) or from impurities of the enriched ^{64}Ni targets (^{55}Co , ^{60}Cu , ^{61}Cu , and ^{62}Cu).⁸²

Spectrophotometric titrations of L_4 with stoichiometric amounts of Zn(II), Co(II), and Ni(II) versus pH showed spectral variations between pH 2 and 12, suggesting a weaker stability of the ML complexes and the possible presence of other species (Supporting Information, Figures S16–S18). The Zn(II), Co(II), and Ni(II) complexes were therefore also studied and characterized by potentiometric titrations versus pH (Supporting Information, Figure S19). For Zn(II), potentiometric titrations pointed to the formation of a single 1:1 (M/ L_4) complex, in line with solid-state and ^1H NMR studies and with the data obtained for Cu(II). However, the formation of an ML_4H species was observed with Co(II) and Ni(II). At basic pH, an additional $\text{ML}_4(\text{OH})$ species was observed with Ni(II). The average values of the stability constants for all the studied cations are summarized in Table 4. Because of very small variations in the spectrophotometric titration of the Zn(II) complex, only the potentiometric titrations were exploited to determine its stability constant. Also, because of the low amount of $\text{Co}L_4\text{H}$ formed (Supporting Information, Figure S21) and the weak spectral variations associated, this stability constant could only be determined by potentiometric technique.

These results clearly showed a strong stability of the Cu(II) complex and a good selectivity of L_4 for Cu(II) compared to Zn(II) < Ni(II) < Co(II), in line with the Irving–Williams series,⁸⁵ with at least five orders of magnitude of difference in the $\log K_{\text{ML}}$ value. Moreover, only the $\text{Cu}L_4$ species was identified and is very stable from pH 2 to 12. The error on the stability constant of the $\text{Cu}L_4$ is due to the absence of control of ionic strength in the batch titration between pH 0 and 1. Errors on the other constants are due to the absence or weakness of charge-transfer bands for Ni(II) and Co(II) that forced us to fit the spectrophotometric data on the ligand bands where the presence of both the protonated species and metal complexes renders the fit more complicated and increases the standard error. The electronic spectra of the complexes (Supporting Information, Figure S20) and the species distribution profiles (Supporting Information, Figure S21) were calculated from the thermodynamic stability constants. The distribution curves show that for all the metal ions, the ML complex is the major species at physiological pH (pH = 7.4). Moreover, the strong stability of $\text{Cu}L_4$ makes it the major species over the whole pH range (pH 2–12), suggesting that this complex would not dissociate due to any change of pH in the human body.⁸⁶ Because of its slow complexation kinetics with Cu(II), coordination with Zn(II), Ni(II), and Co(II) was not studied.

Electrochemical Behavior of the Complex $\text{Cu}L_4$. In vivo dissociation of Cu(II) complexes often occurs through the reduction to Cu(I) and subsequent demetalation. As a consequence, complexes should possess a reduction potential below the threshold for in vivo reduction, estimated to -0.4 V (vs NHE). We thus performed CV studies at different pH on the $\text{Cu}L_4$ complex (Figure 7 and Supporting Information, Figure S22).

Between pH 4 and 9, quasi-reversible processes were observed both in reduction and oxidation. A single redox couple was identified in this pH range, corresponding to Cu(II)/Cu(I) ($E_{\text{red}} = -0.56$ V vs NHE). This is clearly indicating the absence of demetalation and suggests that our complex is able to stabilize both Cu(II) and Cu(I) in this pH range. Such behavior is all the more remarkable considering it is at the origin of the reputation of cross-bridged systems, such as CB-TE2A ($E_{1/2} = -0.88$ V vs NHE), as very strong ligands for copper. Similar behaviors were also observed for other bispidone derivatives⁴² and for NO1PA2PY ($E_{\text{red}} = -0.518$ V vs NHE)³³ and CB-TE1PA ($E_{1/2} = -0.86$ V vs SEC).³⁰ Quasi-reversibility was also verified by varying the scan speed at fixed pH and linearization of $i_{\text{pc}} = f(v^{1/2})$ (Supporting Information, Figure S23). The E_{red} value of -0.56 V versus NHE is placing ligand L_4 well below the estimated -0.40 V (NHE) threshold for typical bioeductants (Supporting Information, Figure S24)⁹ and below Cu(II) complexes with bispidones L_0 ($E_{\text{red}} = -0.323$ V vs NHE) and HZ2 ($E_{\text{red}} = -0.225$ V vs NHE).⁴² More stable bispidine ligands have been reported more recently; however, redox potentials were measured in acetonitrile solutions and therefore cannot be compared with our system.⁴⁰ With such a low redox potential, our complex should thus not be subject to reduction, demetalation, or dismutation under physiological conditions. More complex phenomena were nevertheless observed in strongly acid or basic media (Supporting Information, Figure S22). At pH = 2.38, a second oxidation wave appears, which is assigned to the Cu(I)/Cu(0) redox couple due to demetalation and release of Cu(I) in solution. Similar results were observed for CuL_5 ($E_{1/2} = -0.48$ V vs NHE, quasi-reversible system, Supporting Information, Figure S25).

Kinetic Inertness of CuL_4 in Acidic Media. Strong candidates for radiopharmaceutical applications exhibit strong stability at physiological pH and, in reductive medium, good selectivity but most importantly, high kinetic inertness toward dissociation.²⁰ The kinetic inertness of a complex is commonly evaluated by following its acid-assisted dissociation in strongly acidic conditions under pseudo-first-order conditions. Providing all other criteria were satisfied, the obtained half-life was shown to be a good gauge of the in vivo stability of ^{64}Cu -labeled chelates.⁸⁹ The decomplexation of the CuL_4 complex in 5 M HClO_4 aqueous solutions at 25 °C were studied under pseudo-first-order conditions and followed by UV–visible absorption spectrophotometry over four months (Figure 8). The half-life value ($t_{1/2} = 110$ d) indicates a high degree of inertness of the complex. The Cu(II) complex with ligand L_6 was also studied in the same conditions and also presents high kinetic inertness ($t_{1/2} = 140$ d at 25 °C, Supporting Information, Figure S26), which can be attributed to the rigid bispidine skeleton. These results are particularly encouraging, and radiolabeling with ^{64}Cu should be performed to evaluate the stability in biological conditions.

The $t_{1/2}$, E_{red} , as well as the pM values at physiological pH ($\text{pM} = -\log[\text{M(II)}_{\text{free}}]$, $[\text{M}] = 1 \times 10^{-6}$ M, $[\text{L}] = 1 \times 10^{-5}$ M, pH = 7.4)²² are important parameters to establish a reliable comparison of the complexation properties of different ligands. A selection is presented in Table 5.

Ligand L_4 displays a stronger affinity constant for Cu(II) than the methyl (HZ2, Chart 2) and the thiophen (L_6) analogues but a weaker one than that of the pyridyl-substituted bispidones L_0 (Chart 1). This is probably due to the higher affinity of the borderline cation Cu(II) for N than for O atoms.

L_4 shows a higher pCu than TETA, which has long been considered as a good chelator for Cu(II).⁸⁹ Higher pCu values have been reported for cyclam, TETA, and H_2DEDPA , but their use is limited by their weak kinetic inertness, which in the case of cyclam and TETA is responsible for transchelation reactions of $^{64}\text{Cu(II)}$ to liver and blood proteins.¹⁷ From these data, we can foresee that ligands L_4 and L_6 are strong candidates to be used for the complexation of ^{64}Cu and ^{67}Cu for radiolabeling applications.

CONCLUSION

The last two decades have been marked by a growing interest in copper radionuclides. This interest is motivated by the need to develop new theranostic agents, in particular, for cancer. The matched pair $^{64}\text{Cu}/^{67}\text{Cu}$ is very attractive for immuno-PET and radiotherapy since ^{64}Cu half-life seems particularly appropriate for targeting antibody, fragments, and other macromolecules with slow pharmacokinetics. A network of cyclotron facilities for the production of ^{64}Cu is being developed, and reliable and cost-effective production routes for ^{67}Cu are under study. A large number of macrocyclic chelates and podants have been and are still studied with the aim to satisfy the very strict requirements for such applications. The new bispidine ligands L_4 presented in this work appear as a very attractive candidate for the design of Cu radiopharmaceuticals. This water-soluble ligand, as well as its derivatives, can be readily obtained in four steps from inexpensive starting materials such as dimethyl 3-oxoglutarate, formaldehyde, methylamine, and glycine. As seen from the X-ray structures of L_1 and the corresponding Zn(II) complex $[\text{ZnL}_1\text{Cl}]$, the chair–chair conformation of the bicyclic rings, together with the cis-symmetrical configuration of the pyridyl substituents, provide a highly preorganized coordination sphere, well-adapted for the coordination of transition metals. This has been confirmed by ^1H NMR studies as well as by a detailed physicochemical analysis of ligand L_4 and its complexation properties with Zn(II), Ni(II), Co(II), and, more interestingly, Cu(II). Fast complexation occurs in strongly acidic media (pH = 1), with a strong affinity toward Cu(II) ($\log K_{\text{CuL}_4} = 19.2(3)$, pCu = 17, pH 7.4) and high selectivity versus Co(II), Ni(II), and Zn(II). Moreover, the complex was found to be remarkably inert regarding reduction (with a reversible redox potential of $E_{\text{red}} = -0.56$ V vs NHE) and acid-assisted dissociation ($t_{1/2} = 110$ d, 5 M HClO_4 , 25 °C). From these results, ligand L_4 is expected to lead to a good chelator for radiolabeling studies with ^{64}Cu . Several functionalization strategies are under investigation to obtain bifunctional analogues for molecular targeting.

ASSOCIATED CONTENT

Supporting Information

1D and 2D NMR spectra, plots of spectrophotometric and potentiometric titration data, calculated electronic spectra, illustrated pH titration data, UV–vis spectra, distribution diagrams, CVs, plot showing influence of scan speed on current intensity at pH 7.4, scales of redox potentials of common biological systems, and crystallographic data for $[\text{ZnL}_5]\text{Cl}$ in CIF format (Ic120801_Zn15). This material is available free of charge via the Internet at <http://pubs.acs.org>.

AUTHOR INFORMATION

Corresponding Authors

*E-mail: aline.nonat@unistra.fr. (A.M.N.)

*E-mail: l.charbonn@unistra.fr. (L.J.C.)

Notes

The authors declare no competing financial interest.

ACKNOWLEDGMENTS

This research was performed in the frame of the project “⁶⁴Cu radiolabeled nanomaterials for diagnostic and radiotherapy” (French ANR JCJC SIMI 7). This work was supported by the French Centre National de la Recherche Scientifique and the Univ. of Strasbourg (UMR 7178).

REFERENCES

- (1) Beyer, T.; Townsend, D. W.; Brun, T.; Kinahan, P. E.; Charron, M.; Roddy, R.; Jerin, J.; Young, J.; Byars, L.; Nutt, R. *J. Nucl. Med.* **2000**, *41* (8), 1369–1379.
- (2) van Dongen, G. A.; Visser, G. W.; Lub-de Hooge, M. N.; de Vries, E. G.; Perk, L. R. *Oncologist* **2007**, *12*, 1379–1389.
- (3) Lee, F. T.; Scott, A. M. *J. Nucl. Med.* **2003**, *44*, 1282–1283.
- (4) Holland, J. P.; Williamson, M. J.; Lewis, J. S. *Mol. Imaging* **2010**, *9*, 1–20.
- (5) Shokeen, M.; Anderson, C. J. *Acc. Chem. Res.* **2009**, *42*, 832–841.
- (6) Brasse, D.; Nonat, A. *Dalton Trans.* **2015**, *44*, 4845–4858.
- (7) Price, E. W.; Orvig, C. *Chem. Soc. Rev.* **2014**, *43*, 260–290.
- (8) Zeglis, B. M.; Houghton, J. L.; Evans, M. J.; Viola-Villegas, N.; Lewis, J. S. *Inorg. Chem.* **2014**, *53* (4), 1880–1899.
- (9) Wadas, T. J.; Wong, E. H.; Weisman, G. R.; Anderson, C. J. *Chem. Rev.* **2010**, *110* (5), 2858–2902.
- (10) Cai, Z.; Anderson, C. J. *J. Labelled Compd. Radiopharm.* **2014**, *57*, 224–230.
- (11) Zeglis, B. M.; Lewis, J. S. *Dalton Trans.* **2011**, *40*, 6168–6195.
- (12) Guérin, B.; Ait-Mohand, S.; Tremblay, M.-C.; Dumulon-Perreault, V.; Fournier, P.; Bénard, F. *Org. Lett.* **2010**, *12* (2), 280–283.
- (13) Ferdani, R.; Stigers, D. J.; Fiamengo, A. L.; Wei, L.; Li, B. T. Y.; Golen, J. A.; Rheingold, A. L.; Weisman, G. R.; Wong, E. H.; Anderson, C. J. *Dalton Trans.* **2012**, *41* (7), 1938–1950.
- (14) Silversides, J. D.; Smith, R.; Archibald, S. J. *Dalton Trans.* **2011**, *40*, 6289–6297.
- (15) Kotek, J.; Lubal, P.; Hermann, P.; Cisarova, I.; Lukes; Godula, T. *Chem.—Eur. J.* **2003**, *9*, 233–248.
- (16) Bass, L. A.; Wang, M.; Welch, M. J.; Anderson, C. J. *Bioconjugate Chem.* **2000**, *11*, 527–532.
- (17) Jones-Wilson, T. M.; Deal, K. A.; Anderson, C. J.; McCarthy, D. W.; Kovacs, Z.; Motekaitis, R. J.; Sherry, A. D.; Martell, A. E.; Welch, M. J. *Nucl. Med. Biol.* **1998**, *25*, 523–530.
- (18) Anderson, C. J.; Pajeau, T. S.; Edwards, W. B.; Sherman, E. L. C.; Rogers, B. E.; Welch, M. J. *Nucl. Med.* **1995**, *36*, 2315–2325.
- (19) Sprague, J. E.; Peng, Y.; Fiamengo, A. L.; Woodin, K. S.; Southwick, E. A.; Weisman, G. R.; Wong, E. H.; Goden, J. A.; Rheingold, A. L.; Anderson, C. J. *J. Med. Chem.* **2007**, *50*, 2527–2535.
- (20) Woodin, K. S.; Heroux, K. J.; Boswell, C. A.; Wong, E. H.; Weismann, G. R.; Niu, W.; Tomellini, S. A.; Anderson, C. J.; Zakharov, L. N.; Rheingold, A. L. *Eur. J. Inorg. Chem.* **2005**, 4829–4833.
- (21) Wong, E. H.; Weisman, G. R.; Hill, D. C.; Reed, D. P.; Rogers, M. E.; Condon, J. P.; Fagan, M. A.; Calabrese, J. C.; Lam, K. C.; Guzei, I. A.; Rheingold, A. L. *J. Am. Chem. Soc.* **2000**, *122*, 10561–10572.
- (22) Boros, E.; Rybak-Akimova, E.; Holland, J. P.; Rietz, T.; Rotile, N.; Blasi, F.; Day, H.; Latifi, R.; Caravan, P. *Mol. Pharmaceutics* **2014**, *11* (2), 617–629.
- (23) Esteves, C.; Lamosa, R.; Delgado, R.; Costa, J.; Desogere, P.; Rousselin, Y.; Goze, C.; Denat, F. *Inorg. Chem.* **2013**, *52*, 5138–5153.
- (24) Boswell, C. A.; Regino, C. A. S.; Baidoo, K. E.; Wong, K. J.; Milenic, D. E.; Kelley, J. A.; Lai, C. C.; Brechbiel, M. W. *Bioorg. Med. Chem.* **2009**, *17* (2), 548–552.
- (25) Sargeson, A. M. *Coord. Chem. Rev.* **1996**, *151*, 89–114.
- (26) Cooper, M. S.; Ma, M. T.; Sunassee, K.; Shaw, K. P.; Williams, J. D.; Paul, R. L.; Donnelly, P. S.; Blower, P. J. *Bioconjugate Chem.* **2012**, *23*, 1029–1039.
- (27) Mume, E.; Asad, A.; Di Bartolo, N. M.; Kong, L.; Smith, C.; Sargeson, A. M.; Price, R.; Smith, S. V. *Dalton Trans.* **2013**, *42* (40), 14402–14410.
- (28) Christine, C.; Koubemba, M.; Shakir, S.; Clavier, S.; Ehret-Sabatier, L.; Saupe, F.; Orend, G.; Charbonnière, L. *J. Org. Biomol. Chem.* **2012**, *10*, 9183–9190.
- (29) Boros, E.; Cawthray, J. F.; Ferreira, C. L.; Patrick, B. O.; Adam, M. J.; Orvig, C. *Inorg. Chem.* **2012**, *51*, 6279–6284.
- (30) Lima, L. M. P.; Halime, Z.; Marion, R.; Camus, N.; Delgado, R.; Platas-Iglesias, C.; Tripier, R. *Inorg. Chem.* **2014**, *53*, 5269–5279.
- (31) Frindel, M.; Camus, N.; Rauscher, A.; Bourgeois, M.; Alliot, C.; Barré, L.; Gestin, J.-F.; Tripier, R.; Faivre-Chauvet, A. *Nucl. Med. Biol.* **2014**, *41*, e49–57.
- (32) Bailey, G. A.; Price, E. W.; Zeglis, B. M.; Ferreira, C. L.; Boros, E.; Lacasse, M. J.; Patrick, B. O.; Lewis, J. S.; Adam, M. J.; Orvig, C. *Inorg. Chem.* **2012**, *51*, 12575–12589.
- (33) Roger, M.; Lima, L. M. P.; Frindel, M.; Platas-Iglesias, C.; Gestin, J.-F.; Delgado, R.; Patinec, V.; Tripier, R. *Inorg. Chem.* **2013**, *52*, 5246–5259.
- (34) Haller, R. *Arzneim. Forsch.* **1965**, 1327–1330.
- (35) Haller, R. *Arch. Pharm. Ber. Dtsch. Pharm. Ges.* **1969**, *302*, 113–118.
- (36) Comba, P.; Schiek, W. *Coord. Chem. Rev.* **2003**, *238–239*, 21–29.
- (37) Comba, P.; Kerscher, M.; Schiek, W. In *Progress in Inorganic Chemistry*; Karlin, K. D., Ed.; John Wiley & Sons, Inc.: New York, 2007; pp 613–704.
- (38) Juran, S.; Wather, M.; Stephan, H.; Bergmann, R.; Steinbach, J.; Kraus, W.; Emmerling, F.; Comba, P. *Bioconjugate Chem.* **2009**, *20*, 347–359.
- (39) Comba, P.; Kubeil, M.; Pietzsch, J.; Rudolf, H.; Sephan, H.; Zarschler, K. *Inorg. Chem.* **2014**, *53* (13), 6698–6707.
- (40) Comba, P.; Hunoldt, S.; Morgen, M.; Pietzsch, J.; Stephan, H.; Wadepohl, H. *Inorg. Chem.* **2013**, *52* (14), 8131–8143.
- (41) Bleiholder, C.; Börzel, H.; Comba, P.; Ferrari, R.; Heydt, M.; Kerscher, M.; Kuwata, S.; Laurency, G.; Lawrance, G. A.; Lienke, A.; Martin, B.; Merz, M.; Nuber, B.; Pritzkow, H. *Inorg. Chem.* **2005**, *44*, 8145–8155.
- (42) Born, K.; Comba, P.; Ferrari, R.; Lawrance, G. A.; Wadepohl, H. *Inorg. Chem.* **2007**, *46*, 458–464.
- (43) Legdali, T.; Roux, A.; Nonat, A. M.; Platas-Iglesias, C.; Charbonnière, L. J. *J. Org. Chem.* **2012**, *77*, 11167–11176.
- (44) Gottlieb, H. E.; Kottlyar, K.; Nudelman, A. *J. Org. Chem.* **1997**, *62*, 7512–7515.
- (45) Mikkelsen, K.; Nielsen, S. O. *J. Chem. Phys.* **1960**, *32*, 632–637.
- (46) *M86-E01078 APEX2 User Manual*; Bruker AXS Inc.: Madison, WI, 2006.
- (47) Sheldrick, G. M. *Acta Crystallogr.* **1990**, *A46*, 467–473.
- (48) Sheldrick, G. *SHELXL-97*; Universität Göttingen: Göttingen, Germany, 1999.
- (49) *M86-E01078 APEX2 User Manual*; Bruker AXS Inc.: Madison, WI, 2006.
- (50) Spek, A. L. *J. Appl. Crystallogr.* **2003**, *36*, 7–13.
- (51) Barnes, N. A.; Brooker, A. T.; Godfrey, S. M.; Mallender, P. R.; Pritchard, R. G.; Sadler, M. *Eur. J. Org. Chem.* **2008**, 1019–1030.
- (52) Nonat, A.; Giraud, M.; Gateau, C.; Fries, P. H.; Helm, L.; Mazzanti, M. *Dalton Trans.* **2009**, 8033–8046.
- (53) *Méthodes d'analyses complexométriques avec les Titriplex*; Merck, E., Ed.; Darmstadt, Germany, 1990.
- (54) Raymond, K. N. *Chem. Eng. News* **1983**, *61*, 4–5.
- (55) Gans, P.; O'Sullivan, B. *GLEE 3.0.15*; Protonic Softwares: Leeds, U.K. and Berkeley, CA, 2005.
- (56) Gans, P.; O'Sullivan, B. *Talanta* **2000**, *51*, 33–37.
- (57) Gans, P.; Sabatini, A.; Vacca, A. *Talanta* **1996**, *43*, 1739–1753.
- (58) Alderighi, L.; Gans, P.; Ienco, A.; Peters, D.; Sabatini, A.; Vacca, A. *Coord. Chem. Rev.* **1999**, *184*, 311–318.
- (59) (a) Gampp, H.; Maeder, M.; Meyer, C. J.; Zuberbühler, A. D. *Talanta* **1985**, *32*, 95–101. (b) Rossoti, F. J. C.; Rossoti, H. S.; Whewell, R. J. *J. Inorg. Nucl. Chem.* **1971**, *33*, 2051–2065. (c) Gampp,

- H.; Maeder, M.; Meyer, C. J.; Zuberbühler, A. D. *Talanta* **1985**, *32*, 257–264. (d) Gampp, H.; Maeder, M.; Meyer, C. J.; Zuberbühler, A. D. *Talanta* **1986**, *33*, 943–951.
- (60) Comba, P.; Kanellakopulos, B.; Katsichtis, C.; Lienke, A.; Pritzkow, H.; Rominger, F. J. *Chem. Soc., Dalton Trans.* **1998**, 3997–4001.
- (61) Haller, R.; Unholzer, H. *Arch. Pharm. (Weinheim, Ger.)* **1970**, 654–659.
- (62) Hough, E.; Hansen, L. K.; Birken, B.; Jynge, K.; Hansen, S.; Hardvik, A.; Little, C.; Dodson, E.; Derewenda, Z. *Nature* **1989**, 338–357.
- (63) Comba, P.; Kerscher, M.; Lawrance, G. A.; Martin, B.; Wadepohl, H.; Wunderlich, S. *Angew. Chem., Int. Ed.* **2008**, *47*, 4740–4743.
- (64) Comba, P.; Lopez de Laorden, C.; Pritzkow, H. *Helv. Chim. Acta* **2005**, *88*, 647–664.
- (65) Börzel, H.; Comba, P.; Hagen, K. S.; Lampeka, Y. D.; Lienke, A.; Linti, G.; Merz, M.; Pritzkow, H.; Tsybmal, L. V. *Inorg. Chim. Acta* **2002**, *337*, 407–419.
- (66) Abada, S.; Lecointre, A.; Déchamps, I.; Platas-Iglesias, C.; Christine, C.; Elhabiri, M.; Charbonnière, L. *Radiochim. Acta* **2011**, *99*, 663–678.
- (67) Coppens, G.; Gillet, C.; Nasielski, J.; Donckt, E. *Spectrochim. Acta* **1962**, *18*, 1441–1453.
- (68) Gottarelli, G.; Samori, B. *Tetrahedron Lett.* **1970**, *11*, 2055–2058.
- (69) Meyer, M.; Frémond, L.; Tabard, A.; Espinosa, E.; Vollmer, G. Y.; Guillard, R.; Dory, Y. *New J. Chem.* **2005**, *29*, 99–108.
- (70) Brandel, J.; Lecointre, A.; Kollek, J.; Michel, S.; Hubscher-Bruder, V.; Déchamps-Olivier, I.; Plata-Iglesias, C.; Charbonnière, L. J. *Dalton Trans.* **2014**, *43*, 9070–9080.
- (71) Gans, P.; Sabatini, A.; Vacca, A. *HYPERQUAD2000*; Protonic Software and University of Florence: Leeds, U.K. and Florence, Italy, 2000.
- (72) *Specfit, Version 1–2*; Spectrum Software Associates: Chapel Hill, NC, 1996.
- (73) Siener, T.; Cambareri, A.; Kuhl, U.; Englberger, W.; Haurand, M.; Kögel, B.; Holzgrabe, U. *J. Med. Chem.* **2000**, *43*, 3746–3751.
- (74) Kuhl, U.; Englberger, W.; Haurand, M.; Holzgrabe, U. *Arch. Pharm.* **2000**, *333*, 226–230.
- (75) Hosken, G. D.; Hancock, R. D. *J. Chem. Soc., Chem. Commun.* **1994**, 1363–1364.
- (76) Fischer, A.; King, M. J.; Robinson, F. P. *Can. J. Chem.* **1978**, *56*, 3059–3067.
- (77) Lomozik, L. *Monatsh. Chem.* **1984**, *115*, 261–270.
- (78) Hathaway, B. J.; Billing, D. E. *Coord. Chem. Rev.* **1970**, *5*, 143–207.
- (79) Abada, S.; Lecointre, A.; Elhabiri, M.; Charbonnière, L. J. *Dalton Trans.* **2010**, *39* (38), 9055–9062.
- (80) Abada, S.; Lecointre, A.; Christine, C.; Ehret-Sabatier, L.; Saupé, F.; Orend, G.; Brasse, D.; Ouadi, A.; Hussenet, T.; Laquerrière, P.; Elhabiri, M.; Charbonnière, L. J. *Org. Biomol. Chem.* **2014**, *12* (47), 9601–9620.
- (81) Szelecsenyi, F.; Blessing, G.; Qaim, S. M. *Appl. Radiat. Isot.* **1993**, *44*, 575–580.
- (82) *Cyclotron Produced Radionuclides: Physical Characteristics and Production Methods*, Technical Reports Series; International Atomic Energy Agency: Vienna, 2009; p. 24, ISSN 0074-1914 ISBN 9789201069085.
- (83) Patel, R. N.; Shrivastava, R. P.; Singh, N.; Kumar, S.; Pandeya, K. B. *Indian J. Chem.* **2001**, *40A*, 361–367.
- (84) Srivastava, H.; Tiwari, D. *Indian J. Chem.* **1995**, *34A*, 550–555.
- (85) Irving, H.; Williams, R. J. P. *J. Chem. Soc.* **1953**, 3192–3210.
- (86) Brooker, C. *Le corps humain: Étude, structure et fonction*; De Boeck Supérieur, 2001.
- (87) Odendaal, Y.; Fiamengo, A. L.; Ferdani, R.; Wadas, T. J.; Hill, D. C.; Peng, Y.; Heroux, K. J.; Golen, J. A.; Rheingold, A. L.; Anderson, C. J.; Weisman, G. R.; Wong, E. H. *Inorg. Chem.* **2011**, *50*, 3078–3086.
- (88) Stigers, D. J.; Ferdani, R.; Weisman, G. R.; Wong, E. H.; Anderson, C. J.; Golen, J. A.; Moore, C.; Rheingold, A. L. *Dalton Trans.* **2010**, *39*, 1699–1701.
- (89) Anderson, C. J.; Dehdashti, F.; Cutler, P. D.; Schwarz, S. W.; Laforest, R.; Bass, L. A.; Lewis, J. S.; McCarthy, D. W. *J. Med. Chem.* **2001**, *42* (2), 213–221.